

Understanding volcanic systems and their dynamics combining field and physical volcanology with petrology studies

Raffaello Cioni, Marco Pistolesi, Massimo Pompilio, Bruno Scaillet

▶ **To cite this version:**

Raffaello Cioni, Marco Pistolesi, Massimo Pompilio, Bruno Scaillet. Understanding volcanic systems and their dynamics combining field and physical volcanology with petrology studies. Forecasting and Planning for Volcanic Hazards, Risks, and Disasters, Chapitre 7, Elsevier, pp.285-328, 2021, Chapter 7 - Understanding volcanic systems and their dynamics combining field and physical volcanology with petrology studies, 10.1016/B978-0-12-818082-2.00007-X . insu-02962335

HAL Id: insu-02962335

https://insu.hal.science/insu-02962335

Submitted on 9 Oct 2020

HAL is a multi-disciplinary open access archive for the deposit and dissemination of scientific research documents, whether they are published or not. The documents may come from teaching and research institutions in France or abroad, or from public or private research centers.

L'archive ouverte pluridisciplinaire **HAL**, est destinée au dépôt et à la diffusion de documents scientifiques de niveau recherche, publiés ou non, émanant des établissements d'enseignement et de recherche français ou étrangers, des laboratoires publics ou privés.

Understanding volcanic systems and their dynamics combining field and physical volcanology with petrology studies

Raffaello Cioni[1], Marco Pistolesi[2], Massimo Pompilio[3], Bruno Scaillet[4]

[1] Dipartimento Scienze della Terra, Università di Firenze, Italy
[2] Dipartimento Scienze della Terra, Università di Pisa, Italy
[3] Istituto Nazionale di Geofisica e Vulcanologia, Sezione di Pisa, Italy
[4] Institut des Sciences de la Terre d'Orléans, Orléans, France

Abstract

Hazard assessment and definition of the eruptive scenarios at active volcanoes are mostly based on the elaboration of a large set of information collected with different disciplines and multiple analytical approaches. We discuss here how the reconstruction of the main processes acting at a volcano during its life should be based on the direct knowledge of its activity and products, in the view that each volcano is characterized by its own «personality». Comparison with analogue volcanoes can add further important information on the expected variability of the different processes, but this should never substitute specific data collection at the volcano of interest. Field volcanology and petrology studies are the base for collecting large datasets on past, recent and on-going activity and products. Based on these data, intensive and extensive physical parameters which control the dynamics of the activity can then be derived through focused physical volcanology investigations. Experimental petrology on the products of well-characterized

eruptions finally returns a set of additional physical and compositional parameters that heavily contribute to enlarge our knowledge of the activity and evolution of a given volcano.

Introduction

Volcanic activity is the result of a complex series of processes at different scales involving magma dynamics in the mantle-crust system. The type of erupted products, and the style of eruptive activity, are deeply controlled by the different processes of magma evolution in time and space. The different stages and the modalities of magma accumulation and transfer at shallow depths in the crust, heat and mass exchange with the surrounding host rocks or from the magma source, and consequent magma crystallization, evolution and eventually degassing, are crucial in controlling the variability of eruptive styles.

Understanding the main characteristics of volcanic activity in terms of style, timing, physical processes and evolution is the key for developing a comprehensive, quantitative assessment of volcanic hazards and for the definition of the range of expected eruptive scenarios at an active volcano. In order to get this complex picture, the volcanic system should be considered in its entireness as a complex system in which the processes controlling the different parts concur to regulate its general behavior. For this reason, various approaches should be combined in order to unravel the complex interplay among the zone of storage, the shallow plumbing system connecting a volcanic system to the surface, the volcanic edifice and the variability of the deposits emplaced during eruptions. The knowledge of location, internal geometry, and history of a volcanic system thus represents the basis for the interpretation of the modalities of magma eruption to the surface. Therefore, when dealing with these aspects, an exhaustive study of the whole volcano should be initially planned, with the goal of being largely representative of the different processes which

47 regulated its history. Field studies, physical characterization and petrological investigations on
48 ongoing eruptions or on past volcanic products can be a powerful and effective tool to investigate
49 the main features of the volcanic system and its variation in time and in space (Fig. 1). These data
50 offer the frame for the interpretation of the geophysical and geochemical signals collected at
51 selected volcanic areas, during quiescent periods, episodes of unrest or eruptions. They serve to
52 define a reliable model for the interpretation of the modalities of reactivation and for the expected
53 variability of eruption styles at active volcanoes.

54 When studying the products of the past activity of a volcano, collection of data of very
55 different types (age, composition, sedimentological features of the deposits, etc.) can be generally
56 carried out at two different scales:

57 - At the scale of the whole volcano history, by collecting data on the different products
58 emplaced through time, in order to gain insights into the temporal evolution of the volcano and its
59 deep and shallow plumbing systems;

60 - At the scale of single eruptions, by looking at the products of selected events to reconstruct
61 in detail the evolution of magma reservoir(s), the processes of reactivation and the dynamics of
62 the eruption.

63 In this chapter we will discuss the different types of approach suggested for defining the
64 evolution of a volcanic system and its general eruptive behavior, using information derived from
65 field volcanology, physical characterization of eruptions and petrology studies. We will discuss
66 first the rationale for the two different scales of observations described above, and the set of field
67 studies and physical data needed to collect different sets of information. This part will be
68 preliminary to the presentation and discussion of the methods used in modern petrology aimed at
69 enlarging our knowledge of volcanic system evolution and behavior. The main objective of this

chapter is to illustrate how the direct knowledge of a single volcanic system is fundamental for understanding its activity and evolution so as to reach a robust assessment of volcanic hazards. The use of data from "analogue" volcanoes worldwide can be useful to derive a first order range of expected styles of activity at a given volcano, but should never substitute specific, focussed research on the volcano of interest.

Reconstructing the evolution of a volcanic system

The main processes which control the life and evolution of a volcanic system are well recorded in the physico-chemical features of the erupted products and in the sedimentological and volcanological characteristics of its erupted products. For this reason, the study of the deposits of past eruptions is a pre-requisite for gaining an in depth understanding of the internal structure of the volcanic system. Eruptive history can be reconstructed through collection of a complex set of information on the products of past eruptions, the time-progression of activity, and the phases of morphological and structural evolution of the volcanic edifice. The basic dataset is composed by geological, volcanological, geochemical and petrological data. The reconstruction of the tectonic setting also allows to frame the volcanic activity in a general picture explaining its evolution with time, the composition of involved magmas and the frequency and type of activity (Crisp, 1984; Wilson, 2007).

Geological mapping and stratigraphic studies

Geological mapping of a volcanic area gives the fundamental framework for interpreting the temporal evolution of the activity and the most important changes in the structure of a volcanic system (Groppelli and Viereck-Goette, 2010). This type of studies should be still considered as a forefront topic, although in the past decade very few resources (both human and economic) have

93 been dedicated to this activity. Moreover, although geological maps exist for various active,
94 quiescent or inactive volcanoes, many of them have been traced in the past using mainly a
95 petrological approach or old volcanological concepts (i.e. in many maps pyroclastic products are
96 often described and grouped under the general, lithological term of 'tuffs", without further
97 information useful to derive their genetic or depositional processes). A complete revision of these
98 maps should be still considered as a priority. For this reason, the production of geological maps in
99 volcanic areas should be addressed toward the compilation of real "volcanological" maps, in which
100 deposits and products are presented and described under a volcanological perspective, with legends
101 and stratigraphic or structural schemes which maximize information on the volcanic evolution.
102 Introduction of unconformity bounded stratigraphic units (UBSU) derived from sequence
103 stratigraphy has been for example proposed at Italian volcanoes by several authors to summarize
104 the volcano evolution, although lithostratigraphic units remain the best way to report and describe
105 the geology of a volcanic area (Groppelli and Viereck-Goette, 2010 and refs. therein). Structural
106 geology data should always complement volcanological maps, as they represent an indispensable
107 piece of information, especially at active volcanoes, to understand their past dynamics as well the
108 expected behavior during future episodes of unrest (Acocella 2007, 2014; Azzaro et al., 2012;
109 Cembrano and Lara, 2009; Tibaldi et al., 2003). Mapping of volcanic areas strongly relies on the
110 reconstruction of a detailed reference stratigraphic sequence, which is a complex and time-
111 consuming task to achieve (Fig. 2; Marti et al., 2018, and refs. therein). This can be acquired only
112 through an extended, detailed field survey of the entire pile of emplaced deposits. In large volcanic
113 areas, with activity from different centers (at local or regional scale), the identification of clearly
114 defined stratigraphic markers in the succession is a primary task, which can be used to correlate
115 the activity of the different volcanic centers and to define the temporal evolution of the activity. In

some cases, stratigraphic data can be integrated with those derived from distal and ultra-distal sites (both marine, lacustrine and terrestrial) where tephra beds are recollected, identified and dated (Pyle et al., 2006; Matthews et al., 2012; Engwell et al., 2014). Only in a few cases, such as at frequently erupting volcanoes in inhabited areas and with a long-lasting written tradition, eyewitnesses' accounts are useful to reconstruct the most recent period of activity and to fill in possible gaps in the stratigraphic sequence related to small-scale eruptions with scarce deposition and/or preservation. The preservation potential for the deposits of past eruptions in fact strongly varies as a function of the general dispersal, thickness and grain-size of the deposits of each eruption (roughly correlated to the intensity and magnitude; Pyle, 2015), and on climate, that may enhance rapid weathering and erosion also of very recent deposits. Moreover, a volcanic area is a highly dynamic morphological system in which short periods of deposition alternate with prolonged periods of erosion and landscape reshaping (Collins and Dunne, 1986; Nemeth and Cronin, 2007; Thouret, 1999). In many cases, the time for the latter is order of magnitudes longer than that during which eruptions occur and products accumulate. These discontinuous dynamics are also amplified by the large variability of frequency and magnitude (considered as proxies for the volume of erupted products) of the eruptions, with the largest, low-frequency events being generally best recorded in the stratigraphic sequence and preserved also in distal sequences with respect to the more frequent, smaller events, mostly dispersed in the proximal sectors of the volcano. All these factors may result in a partial, incomplete geological record of the past activity and need to be carefully evaluated when trying to reconstruct a detailed history of a volcanic system (Brown et al., 2014; Newhall and Self, 1982).

Geochronological studies

Radiometric dating of the deposits is an essential tool that should always accompany the stratigraphic reconstruction, giving an absolute measure of the timing for the different processes (e.g., eruptions, magma evolution, edifice building). A detailed, high resolution dataset (both in terms of precision of age determination and number of dated events) is vital, as it can reveal different trends in the activity, such as temporal clustering of eruptions, or variability of frequency with time (Fig. 3). Geochronological data are strongly unevenly distributed between the different volcanoes worldwide, and totally lacking at many important active volcanic systems, especially in remote areas (Simkin et al., 1981). In most cases, available absolute ages derive from inhomogeneous datasets obtained with different techniques and at different laboratories, often resulting in discordant results. In addition, many available geochronological datasets suffer from a lack of systematic sampling approach with respect to the eruptive history. Time-related reconstructions at the scale of the entire volcanic system should be planned together with geological mapping and stratigraphic investigations, in order to systematize data collection.

Physical characterization of eruptions

Physical characterization of volcanic eruptions should strongly rely on the basic geologic information at the scale of the volcano. These studies involve detailed stratigraphic reconstructions of the deposits of single eruptions, as well as their areal dispersal and the derivation of the main physical parameters which can help eruption classification and understanding of the main processes acting during eruptions (Bonadonna et al., 2015, 2016; Carey and Sparks, 1986; Mastin et al., 2009). At the scale of the whole volcanic system, deposit studies are fundamental to assess the variability of the eruption scenarios shown by the volcanic system in its history (Table 1; Cioni et al., 2008). Together with the information from absolute dating and the time evolution of the volcanic activity (both at short and long time-scales), these combined datasets represent the basic

source to prepare informed and reliable hazard maps and emergency plans. In the recent years, the definition of event trees for the expected evolution of the activity at a given volcano (Newhall and Hoblitt, 2002) has become a common practice in volcanology. This type of theoretical scheme, which summarizes the expected progression of events before a volcanic crisis, is more robust if elaborated with a case-by-case approach, using all the geological and volcanological information available at a given volcanic system (Neri et al., 2008; Marti et al., 2008).

Petrology and geochemistry of erupted products

Petrology and geochemistry of erupted products represent other important aspects to be explored in order to get a complete view of a volcanic system and of its evolution. To depict exhaustively magmatic evolution with time, these data should derive from a systematic collection deeply based on the volcanological and geochronological framework built for that system. This is not the case for data currently available at many volcanoes worldwide, that often suffer problems of underrating of specific phases of activity. Petrological and geochemical studies, coupled with experimental constraints (see sections below), give first order information about the depth of the different parts of the magma storage system and its possible migration with time (e.g., Gardner et al., 1995; Scaillet et al., 2008). They can also allow to define the conditions of magma stalling, crystallization and evolution at depth, or they can inform about the modalities of pre- and syn-eruptive magma ascent to surface (Blundy and Cashman, 2008; Rutherford, 2008). The reconstruction of the evolution of a volcanic system gives the possibility to understand the overall compositional variability shown by the products and to frame their temporal progression. In many cases, it is possible to define cycles of volcano evolution associated to differences in the composition of the erupted magma (Fig. 4). Important information on the depth of the different portions of the volcanic system and on the interaction between magma and host rocks can also be

184 derived from the petro-mineralogical study of lithic fragments ejected during the different
185 explosive events (Di Rocco et al., 2012; Fulignati et al., 2004). Similarly, deep-derived nodules
186 are often found in lavas or pyroclastics, opening a window onto source mechanisms of magma
187 generation, migration and fragmentation at a specific volcano. All these aspects will be discussed
188 in detail in a following section.
189

190 ## Studying single-eruption sequences

191 Important data on eruption processes and eruptive dynamics can be extracted from the
192 detailed study of the products erupted during single eruptions. In this case, the indispensable
193 dataset is represented by the accurate description of the sequence of eruptive products, acquired
194 through detailed stratigraphic, sedimentological and laboratory analyses of the deposits. Different
195 problematics arise in the study of the products of effusive vs. explosive eruptions.
196 Effusive eruptions are generally characterized by the occurrence, often contemporaneous, of lava
197 emission and small-scale explosive activity. Unless in the presence of direct observations of the
198 eruption, the stratigraphic relationships between the products of these two types of activity are
199 often not simple to resolve in the field, due to different dispersal and, often, to the multi-vent
200 character of these eruptions. Sample collection from lava flows, lava flow fields or lava domes is
201 generally less problematic with respect to pyroclastic material due to the generally narrower, more
202 regular dispersal. However, while in pyroclastic products it is generally straightforward to
203 recognize directly in the field the sequence of deposition (and hence eruption) of the deposits, this
204 can be very difficult in complex, long-lasting, often multi-vent past effusive eruptions. Beside this,
205 samples representative of the entire course of the effusive activity can be very difficult to obtain,
206 as magma erupted during the first phases of an effusion can become rapidly inaccessible, unless

207 they are preserved (and still recognizable) at specific locations in the flow, such as at the front or
208 along the lateral levees.

209 Explosive eruptions often result in a complex sequence of deposits, in terms of type (tephra
210 fall, pyroclastic density currents, etc.), dispersal and stratigraphic relationships. Detailed
211 stratigraphy is the first step to trace time and space evolutions of the different deposits, These
212 studies are also the base for the preparation of tephra dispersal maps (isopach, isopleth maps) for
213 the different deposits that can be used to define several extensive (e.g., volume and mass of erupted
214 magma, amount of xenolithic material) and intensive parameters (e.g., plume height, mass flow
215 rate, clast ejection velocity, velocity and dynamic pressure of pyroclastic density currents) of the
216 eruption (Carey and Sigurdsson, 1986; Cioni et al., 2000; Pistolesi et al., 2015, 2017; Todde et al.,
217 2017). The knowledge of all these parameters enables a parameterization of the different types of
218 eruptions which occurred during the life of a volcanic system, thus allowing to relate eruption
219 dynamics with the general features of the volcanic system (magma composition and rheology,
220 rates of magma feeding and evolution, depth and size of magma reservoirs). For an active volcano,
221 this dataset can be successfully used to the assess a range of representative eruption scenarios, to
222 understand its general style of activity (and time evolution) and to build an effective hazard
223 assessment framework (Tab. 1; Cioni et al., 2008).

224 ***Sampling strategies for pyroclastic deposits***

225 The collection of a large set of representative samples for different types of explosive
226 eruptions commonly needs a combination of preparatory studies to be carried out (e.g., selection
227 of the outcrops, sampling strategy). The choice of sampling strategy should always be preceded
228 by a preliminary characterization of the stratigraphy, dispersal, thickness variation and volume of
229 the eruption (e.g., Fisher and Schmincke, 1984; Cas and Wright, 1987; Thordarson et al., 2009;

230 Gurioli et al., 2015). Volcanic plumes which form during explosive eruptions are in fact complex
231 systems and their properties do not vary linearly with the main eruption parameters. The external
232 variables such as wind direction and velocity add further complexity to the tephra sedimentation
233 (i.e. clast-type distribution). Particularly when dealing with recent or ongoing eruptions, sampling
234 should be preceded by an accurate field analysis of the deposits. On this basis, the strategy should
235 consider deposit variability and key locations which synthesize the whole eruptive sequence. Once
236 defined the suitable outcrop(s), an inspection of the base-to-top variability is needed to assess syn-
237 eruptive wind direction or eruption intensity changes. In case of important lithologic and
238 sedimentologic vertical variability (e.g., grain-size, color, density/vesicularity, general
239 morphology, vesicle shape and crystallinity) at the outcrop scale, the identification of different
240 layers is needed prior to collection, eventually sampling each tephra layer at different equivalent
241 locations rather than collecting all samples at a single outcrop (Fig. 5). This is because
242 sedimentation from volcanic plumes is affected by clast size, shape and density (Bonadonna et al.,
243 1998; Pfeiffer et al., 2005; Barsotti et al., 2008; Eychenne et al., 2013), and thus single exposure
244 sampling may affect relative proportions within the deposit of the sampled material which can
245 vary with distance from the vent.
246 While the textural and sedimentological clast variability can be studied at a single outcrop, the
247 relative proportions between the different components of the deposit should be investigated across
248 the whole deposit dispersal by integrating outcrops and sampling at different distances from the
249 vent. Variability of juvenile clasts can be related to inhomogeneous magmatic sources
250 (mixing/mingling processes) or to different syn-eruptive conditions of degassing and
251 crystallization. Sampling is thus particularly crucial when dealing with petrological investigations,
252 which should ensure the representativeness of the collected juvenile fractions for analytical studies

as well as low to absent alteration degree. In the presence of a large variability of juvenile clasts, sampling should be followed by componentry analysis of the clasts population in order to obtain homogenous sub-sets of samples before further analyses (e.g., sample grinding for powders, thin sections). The accurate analysis of proximal deposits can reveal the presence of important, although thin and often poorly dispersed, deposits related to the opening phases of the eruption. The sampling and study of the products of these phases can give important insights into the mechanisms triggering the eruption and accompanying the onset of magma ascent to the surface (Cioni et al., 2000; Sulpizio et al., 2010), as well as the complex processes of magma-rock interaction during the final upward migration of the feeder dyke (Pistolesi et al., 2015).

Componentry of pyroclastic deposits

Pyroclastic deposits are characterized by the presence of clasts derived from the fragmentation of a range of products of different sources, which are distinguished as juvenile and accessory, xenolithic material (Fisher and Schmincke, 1984). Juvenile material represents the magma actively driving the eruption, and most of the petrologic studies are obviously performed on this type of material. The detailed examination of the different types of clasts present in the products of a pyroclastic eruptions can be an incredibly prolific source of information on the different processes affecting magma during an eruption. Microanalytical and textural studies of the fragments are useful to identify the final processes of magma ascent and have been largely used also to indirectly derive the rates of magma ascent, degassing and crystallization (Cashman, 1992; Cashman and Blundy, 2000). Identification of juvenile clasts with different composition in a same eruption, even at a same stratigraphic level or within a single clast, are fundamental to characterize pre-eruptive states of the magma, the existence of compositional gradients in the magma reservoir and the temporal sequence of magma extraction during an eruption.

During eruption, or under pre-eruption conditions, changes in the final composition of the melt phase can be induced by complex processes such as crystallization, assimilation of country rocks, or mixing among different magmatic melts. Magma mixing is often suggested as one of the most common triggers of eruptive activity (Sparks et al., 1978).

If juvenile material is the main, direct source of data about the state of the magma before an eruption, accessory material (accidental or cognate clasts; Fisher and Schmincke, 1984) brings precious information about rocks hosting the volcanic system (contact portions of the reservoir, conduit, crater area) and all kinds of interaction between magma and the host rocks (metasomatic and thermo-metamorphic rocks from the magma reservoir/host rock shell, different kinds of magma cumulates). In case of large eruptions, the combined study of stratigraphy and componentry of the deposits is also used to estimate the dimension of the eruptive magma conduit/crater system and the timing for caldera collapse that may eventually occur.

Internal variability in the products of an effusive eruption

Differently from pyroclastic deposits, the products of effusive activity are almost completely dominated by juvenile magma; mafic lavas are generally strongly homogeneous, mainly due to the low viscosity (also after near complete degassing of the magma) that favors a rapid hybridization of different melts in mixed systems or the rapid disappearance of internal compositional gradients. In such cases, information of the interaction of the magma with different melts is only preserved in the phenocryst population, that can give first-hand information on the physical and chemical conditions of magma evolution. In particular cases, the low viscosity of mafic magmas can result in high ascent rates to the surface, and the ensuing lava flows are characterized by the presence of high-density, crystal-rich, mafic nodules of different size (from mm- up to dm-sized) that may give information both on deep-seated crystallization processes or even on the mantle source.

Effusive activity of silicic magmas, forming lava domes or poorly mobile flows (coulées, tholoids, obsidian flows, etc.), often results in more heterogeneous products, as the high viscosity of the melt-crystal system tends to preserve traces of any interaction of the magma with other melts or rocks, and to show physical mingling instead of chemical hybridization between different magmatic melts with contrasting rheological features. In this case, it is very common to observe a variety of enclaves (Bacon, 1986) that reveal, with their composition and texture, the origin and dynamics of mixing at depth.

Petrological constraints to magma genesis and evolution

The journey of magmas from the mantle source to the surface can be very complex owing to the heterogeneity of the lithosphere and the variability of tectonic regime (Cashman et al., 2017; Scandone et al., 2007). Direct evidence of the geometry and extension of volcanic plumbing systems are mainly derived from geological investigations carried out on ancient dissected volcanic centers or exhumed crustal sections. High resolution seismic profiles or crustal tomography can also provide a variably detailed picture of the extension and complexities of the plumbing system. These methods in most cases provide only a static representation of the spatial complexity of the plumbing system and notwithstanding recent advances on 4D seismic tomography, quite often fail in detailing the physico-chemical parameters at work. More generally, geophysical information is restricted to eruptions that have occurred in the last decades (i.e. accompanying the deployment of geophysical networks). Conversely, a basic assumption of petrological investigations is that compositional and textural variability revealed by petrological methods reflects changes in physical (e.g., pressure, temperature) and chemical (e.g. fO_2) parameters during magma ascent, storage and eruption.

Information on the pre-or syn-eruptive evolution of magmas is generally preserved in their compositional and textural features. For example, crystals and melts provide information about cooling, crystallization, contamination and mixing history, vesicles and melts on volatile content and degassing dynamics.

Whatever the research approach used (at the scale of the entire volcano, or restricted to single eruption sequences), petrological studies should be applied to the products in order to extract information on the main processes that controlled magma genesis and evolution, as well as to define the main compositional differences of the erupted products.

In general, key information about the magmatic system that petrology can provide include:

- The nature and the composition of the magma source;
- The physical and chemical conditions of magmatic processes;
- The dynamics of magmatic processes;
- The timescales for magma crystallization and degassing.

To obtain the above information, volcanologists collect petrological and textural data on natural rocks and their components and interpret these data on the basis of experiments and thermodynamic/ physical models.

The nature and composition of the magma source

Nature and composition of the magma source are mainly investigated via isotope geochemistry on primitive melts and/or on deep-seated xenoliths entrained upward by the magma. Texture and mineral assemblage of xenoliths, once modifications occurring during ascent are filtered out, bear evidence of the nature of the source (Armienti et al., 2013, Corsaro et al., 2009b, Pichavant et al., 2009, Wright & Klein, 2006). By definition, primitive melts are close to the composition of melts in equilibrium with the mantle mineralogy. Criteria for recognizing the

attainment of the equilibrium are based on the K_d of melt-olivine equilibria, assuming that olivine with Fo_{90} is the fundamental component of a residual peridotite. Primitive melts are rare and recognizable as melt inclusions (MIs) trapped in mafic minerals as olivine or pyroxene (Grove et al., 2002; O'Hara & Herzberg, 2002; Pichavant et al., 2002, 2011; Schiano, 2003; Asimow et al., 2004; Green et al., 2004; Smith & Leeman, 2005; Streck et al., 2007).

In most central volcanoes, primitive melts reach the surface only if the characteristic time of transport/ascent through the crust is short enough (highly buoyant magmas) that stopover, cooling or crystallization in the crust are reduced and interaction or mixing with shallow residing magmas is limited (Corsaro & Pompilio 2004a; Coltelli et al. 2005; Kamenetsky et al. 2007).

At some volcanoes (e.g., Etna, Teide or Pantelleria) these conditions are more easily met during flank eruptions, when feeder dykes bypass the central plumbing system. Radiogenic isotopic ratios (Sr, Nd and Pb systematics) and ratios between stable isotopes of noble elements (e.g. Helium) carry information on the geochemical evolution and modification of the source (e.g. metasomatism) since these ratios are not modified during melting, crystallization or degassing (Tonarini et al., 2001; Francalanci et al., 2004, 2007; Tommasini et al., 2007; Pietruszka et al., 2015; Corsaro & Métrich, 2016; Di Renzo et al., 2018). The knowledge of the composition of primitive magmas that feed crustal reservoirs and of their variability in time is crucial for determining the compositional evolution of crustal reservoirs.

Defining physical and chemical parameters of magmatic processes

At almost every stage of magma migration through the crust, cooling and crystallization can take place to some extent. If crystals are preserved in the erupted magma, the whole history can be deciphered and physical and chemical parameters relevant to magmatic processes estimated (Jerram et al., 2018). In the scientific literature of the last 40 years, thermodynamic modeling of

368 phase equilibria between liquid, gas and solid phases has been largely employed to estimate
369 pressure and temperature at which magmatic processes occur (Ghiorso & Sack, 1995; Ghiorso &
370 Gualda, 2015; Gualda et al., 2012). This important advancement has been possible thanks to the
371 large improvement of microanalytical techniques, that allowed the accurate compositional and
372 textural analysis of single phases at a spatial resolution of few microns, and to a wealth of new
373 experiments on natural and synthetic materials allowing a fine tuning of general models, and their
374 application to the knowledge of the plumbing system of a single volcano.
375 A huge number of case-histories appearing in the scientific literature can be cited, however the
376 best and more accurate results are those derived from the study of the products of volcanoes that
377 erupted frequently or during long periods in the last decades (e.g., Etna, Kilauea, Stromboli, Piton
378 de la Fournaise, Mt. Saint Helens, Monserrat) or those for which detailed field studies allowed to
379 reconstruct with a good approximation single key eruptions (e.g., Vesuvius, Santorini) or a large
380 part of the eruptive history (Putirka, 1997; Corsaro & Pompilio, 2004b; Del Carlo & Pompilio,
381 2004; Corsaro et al., 2007, 2009a, 2012, 2014; Peltier et al., 2009; Mollo et al., 2015; Giacomoni
382 et al., 2016, Perinelli et al., 2016; Di Renzo et al., 2018). Pressure and temperature of magma
383 evolution often derive from accurate studies of fluid and MI, as testified by a huge literature
384 starting from the seminal work of Roedder (1979) up to the recent reviews of Kent (2008), Métrich
385 and Wallace (2008) and Moore (2008). In particular, MIs trapped in crystals in equilibrium with
386 the magma driving the eruption can preserve their history of crystallization, recording the temporal
387 variation of the composition and volatile content of magma and giving also the possibility to
388 measure the trapping temperature (Roedder, 1979; Lowenstern, 2001). Volatile content of MI has
389 been often used for estimating the minimum pressure of crystallization, assuming volatile
390 saturation in the melt, so allowing to reconstruct the possible geometry of a plumbing system (e.g.,

391 Pamucku et al., 2015; Métrich et al., 2010; Fig. 6). MI studies must be always accompanied by
392 detailed petrological investigations in order to shed light on the significance of the different hosting
393 phases, and on the possible post-entrapment changes of the melt by host crystallization, MI
394 maturation and degassing, or melt-crystal diffusion (Nielsen et al, 1998).

395 ***Dynamics of magmatic processes***

396 Once assessed where the magma is stored within the crust, it is essential to understand what
397 happens within these stable or short-lived magmatic reservoirs, if some interaction occurs with the
398 host rocks, if and in which proportion magmas mix together or with assimilated crustal material,
399 and if liquid, solid or gas phases separate or accumulate.

400 Classical methods embrace compositional investigations on bulk rocks or on single phases, using
401 information derived from radiogenic isotopes and trace elements. Some examples include recent
402 eruptions or eruptive periods of well-known volcanoes (Pompilio et al., 2011; Meletlidis et al.,
403 2012 ; Troll et al., 2012; Marti et al., 2013; Longpré et al., 2014; Del Moro et al., 2015, Meletlidis
404 et al., 2015, Di Renzo et al., 2018). Textural analyses including both descriptive (e.g., habitus,
405 shape) and quantitative information derived from crystal or vesicle size distributions have been
406 also largely employed, in most of active volcanoes, thanks to the tremendous recent development
407 of image analysis techniques. A combined textural and compositional analysis of fine-grained
408 pyroclasts (ash and lapilli) can give clues on magmatic processes within the plumbing system,
409 such as crystallization and degassing (Hammer et al., 1999, 2000; Blundy and Cashman, 2001;
410 Taddeucci et al., 2004; Schiavi et al., 2006, 2010; D'Oriano et al., 2011; Pompilio et al., 2017).

411 A new original and promising approach at the scale of single crystals is the system analysis
412 (Fig. 7) introduced by Kahl et al. (2011). The basic assumption is that the growth of a sector of a
413 crystal records the crystallization process within a given magmatic environment. A magmatic

414 environment (ME) can be generally defined as a portion of the magmatic plumbing system (not
415 only restricted to the magma reservoir) characterized by a distinctive set of intensive
416 thermodynamic variables (e.g., temperature, pressure, melt composition, water content, and
417 oxygen fugacity). Considering that crystal growth occurs sequentially from core to rim, it can be
418 assumed that the compositions at the rim record the latest magmatic environment while the inner
419 sectors record progressively older environments. Thus, the chemical stratigraphy recorded in the
420 compositional zoning patterns can be used to track the evolution of different magma batches
421 through distinct magmatic environments. However, the interpretation of the patterns of zoning
422 within crystals of the same eruption is not simple, but a system analysis plot (Fig. 7) can clarify
423 the relationships between diverse magmatic environments.

424 ***Timescales for magma crystallization and degassing***

425 Most of intensive thermodynamic variables (e.g., pressure, temperature, volatile content and
426 composition) pertaining to magmatic environments are derived assuming equilibrium conditions
427 and ignoring the kinetics of the processes. In this way, the temporal information that can work as
428 "sync-signal" between petrology and other geophysical signals, is missing. Only in the last two
429 decades, the "re-discovery" of the kinetics of magmatic processes has allowed to obtain robust and
430 precise estimation of timescales, allowing correlation between different signals. Such new
431 petrological techniques include crystal and vesicle size distributions, multi-element diffusion
432 chronometry, and measurements of short-lived isotopes (Hawkesworth et al., 2004; Cooper and
433 Kent, 2014; Petrone et al., 2014).

434 Information on the kinetics of the crystallization or degassing derived by crystal or bubble size
435 distributions have been largely employed to obtain the timescales of storage and ascent of magmas.
436 After the precursory work of Marsh (1988), these techniques have been applied to several

437 volcanoes with different compositions and mineral assemblages (Cashman and Marsh, 1988;
438 Mangan, 1990; Cashman, 1992; Hammer et al., 1999; Zieg & Marsh, 2002; Taddeucci et al., 2004;
439 Zellemer et al., 2005; Higgins, 1996; 2006; Armienti, 2008; Salisbury et al., 2008; Higgins &
440 Roberge, 2007; Morgan et al., 2007a; Proussevitch et al., 2007; Fornaciai et al., 2015; Jerram et
441 al., 2018). In order to recover accurate temporal information from a quantitative textural analysis
442 it is necessary to have a robust estimate of kinetic parameters such as growth and nucleation rates
443 and their relationships with pressure, temperature, undercooling and composition (Armienti,
444 2008). Similarly, the modeling of the diffusive modification of zoning profiles in mineral provides
445 information on the timescale of melt transfer through the plumbing system. For this reason,
446 diffusion modeling is being increasingly used to obtain timescales of individual magmatic
447 processes or sequences of processes. Early applications include the study of eruption of Vesuvius,
448 Santorini, Etna, Mount St. Helens, and most of them include correlation with geophysical signals
449 useful for volcano hazard monitoring (Zellmer et al., 1999, 2003, 2005; Morgan et al., 2007b; Kahl
450 et al., 2011, 2013, 2015, 2017; Charlier et al., 2012; Druitt et al., 2012; Marti et al., 2013;
451 Chamberlain et al., 2014; Albert et al., 2015, 2016).
452

453 ## Experimental constraints on volcano evolution and eruption dynamics

454 As explained above, the petrological study of erupted products can give invaluable
455 information about processes occurring at depth and about the nature of magmas involved in the
456 eruptive mechanisms. In order to correlate such an information with physical inferences made from
457 the study of volcanic deposits it is essential, however, that the petrological information is placed
458 into a robust and quantitative pressure-temperature framework. This is the reason for carrying out
459 experiments in the laboratory, whose prime aim is the replication of essential petrological

460 attributes which are preserved by juvenile material ejected during the eruption, under carefully
461 controlled intensive parameters (P, T, volatiles etc.). It is therefore vital that experimental efforts
462 come only when an in-depth field and petrological knowledge is available, so that the laboratory
463 work is performed on relevant and representative rock types and under naturally constrained
464 physical conditions.

465 Experiments that can be done are of various sort: (1) phase equilibria, (2) volatile solubilities,
466 (3) mixing/interaction experiments, (4) decompression experiments, and (5) measurements of
467 physical properties of rocks and magmas. All these experiments are done for durations which can
468 be very short compared to the timescales attending the construction of volcanic edifices: typically,
469 a stratovolcano building may last several 100 kyrs, a period mirroring that of the reservoir lying
470 below, while experiments are carried for durations varying between minutes/hours at high
471 temperature (>1000°C) up to several weeks in the low end of the terrestrial temperature silicate
472 magmas spectrum (ca 600°C). Yet, fortunately for that matter, pre-eruptive or syn-eruptive
473 phenomena often occur on short time scales, i.e. they can, for the most part, be directly simulated
474 by laboratory experiments under the right P-T conditions and using the natural magma as starting
475 material. Asides from the selection of starting material, in order to be relevant to the natural
476 context, experiments need to be carried out in the correct order: first, phase equilibria which set in
477 the general scene, in particular the broad P-T field of magma storage and evolution, and then the
478 dynamic experiments simulating the process (i.e., decompression, mixing,
479 assimilation/contamination/interaction).

480 ***P-T conditions of magma evolution: phase equilibrium studies***

481 The most common as well as standard approach of experimental petrology studies includes
482 the elaboration of phase relationships at various pressure, temperature and volatile contents. This

483 approach defines the stability fields of the major and minor mineral phases as a function of P, T
484 and melt volatile content (Fig. 8). These data are fundamentally aimed at testing to what extent
485 crystal-liquid equilibria were prevailing in the reservoir prior to eruption, and they allow setting
486 the so-called pre-eruptive conditions. When such an approach is successful, i.e. when experiments
487 can define a range of P-T-volatiles conditions under which the nature, proportion and composition
488 of main phases (including liquid/glass) are reproduced, then it is reasonable to conclude that before
489 eruption the reservoir was at or near equilibrium. Conversely, inability to reproduce the
490 phenocrysts assemblage under a "reasonable" set of P-T-volatiles conditions likely points to
491 disequilibrium, whose cause could be occurrence of magma mixing or coexistence of various
492 phenocrysts having precipitated at different conditions (generally depth/pressure, or temperature)
493 before eruption.

494 Application of the above approach on well selected eruptions (and samples) produced by a
495 single volcano allows one to infer the time evolution of magma storage conditions (Fig. 8). This
496 is crucial since geophysical surveys can only probe the present-day state of the plumbing system,
497 which is the integrated result of all events having occurred so far. The working out of the pre-
498 eruptive conditions of the last event is likely to inform about the state of the reservoir most closely
499 approaching that of present-day conditions, except if the repose time since that event is very long.
500 Not all magmas erupted allow robust estimates via phase equilibrium data to be extracted however,
501 since that method depends on the variance (number of different phases) of the system under
502 consideration. An extreme case is provided by an aphyric lava or obsidian in which the lack of
503 phenocrysts prevents the simple test of crystal-liquid equilibrium. Also, some compositions are
504 saturated with the same phase assemblage over a large range of P-T-volatiles conditions, making
505 such an approach relatively imprecise. In such a case, the search for melt-inclusions trapped in

506 phenocrysts provides a powerful assist to the definition of pre-eruption conditions, as explained
507 below. In general, however, the phase equilibrium approach has proved to be very useful in
508 providing first order P-T-volatile conditions on a number of reference volcanoes as Mt. St. Helens
509 (Rutherford et al., 1985; Gardner et al., 1995), Mt Pelée (Martel et al., 1998; Pichavant et al.,
510 2002), Vesuvius (Scaillet et al., 2008; Pichavant et al., 2014), Santorini (Cottrell et al., 1999,
511 Cadoux et al., 2015; Andujar et al., 2015, 2016), Tungurahua (Andujar et al., 2017), Pinatubo
512 (Scaillet and Evans, 1999).

513 Phase equilibria provide not only a consistent picture of the stability of different phases but
514 they also furnish fundamental data on crystal-crystal or crystal-melt equilibrium partitioning for
515 some key elements (Fe, Mg, Cl, F etc.). Firstly, these allow to evaluate for each crystal pair or
516 isolated individual the equilibrium status with respect to its immediate surrounding. Secondly,
517 combined with thermodynamic principles, these data allow derivation of a variety of hygro-oxy-
518 thermo-barometers which allow to further refine the determination of intensive parameters. The
519 Fe-Ti oxide oxythermometer is certainly one of the most popular and accurate crystal-crystal
520 equilibrium (e.g., Andersen and Lindsley, 1993; Ghiorso and Evans, 2008; Evans et al., 2016)
521 which calculates temperature to perhaps better than 20-30°C and fO_2 to within 0.3 log units.
522 Another similarly powerful and accurate assemblage is the two-feldspars thermometer (e.g.,
523 Fuhrman and Lindsley, 1988). The plagioclase-liquid hygrometer has been shown to be of great
524 assist for inferring dissolved water content of pre- to syn-eruptive melt (Waters and Lange, 2015).
525 Amphibole composition also varies widely as a function of phase assemblage, melt composition
526 and P-T-fO_2-fH_2O conditions, which has led to many empirical parametrizations (e.g., Johnson
527 and Rutherford, 1989; Ridolfi et al., 2010; Putirka, 2016). Apatite, which is a ubiquitous accessory
528 mineral in magmas, is being increasingly used as a monitor of melt volatile contents, the focus

529 being on halogens and sulfur species (e.g., Parat and Holtz, 2005; Webster and Piccoli, 2015).
530 Whenever possible, combination of phase relationships with crystal-crystal and crystal-liquid
531 partitioning, as well as with MI data, should be the strategy of choice to provide robust constraints
532 on the conditions of magma evolution and storage.

533 ***Constraints to magma degassing: volatile solubilities***

534 This part represents an important strand of the experimental approach, owing to the strong
535 pressure dependence of volatiles concentration in silicate melts with pressure, and the important
536 role that volatiles play in driving volcanic eruptions. Since the early developments of experimental
537 petrology, determining the solubilities of H_2O and CO_2, the two most abundant species of
538 magmatic gases, has been a priority for the community (e.g., Blank et al 1993; Dixon et al., 1995;
539 Lesne et al., 2011; Shiskhina et al., 2014). These works have largely shown that water solubility
540 is much greater than that of CO_2 (Fig. 9a), hence the exsolution of the two species varies widely
541 with pressure and the bulk of water is exsolved from the silicate liquid at much lower pressure than
542 that of CO_2. While the compositional control on volatile solubilities is demonstrable, it remains
543 relatively small for water but appreciable for CO_2. Experimental data gathered over the last three
544 decades have allowed the development of multicomponent solubility models (e.g., Newman and
545 Lowenstern, 2002; Papale et al., 2006; Burgisser et al., 2015) whose prime use is the determination
546 of the pressure of magma-gas saturation as a function of dissolved H_2O and CO_2 contents
547 (Anderson et al., 1989). Application of these models to MIs enables one to calculate minimum
548 pressures for those melt aliquots, which can be compared with pressures inferred from phase
549 equilibrium considerations or geophysical constraints. Refinement of this method includes the
550 incorporation of other volatile species, in particular SO_2 and H_2S (e.g., Moretti et al., 2003;
551 Clemente et al., 2004; Lesne et al., 2015) or halogens (Alletti et al., 2012). In general, however,

552 the partial pressures of H_2O and CO_2 represent more than 90% of the total pressure. An important
553 output of volatile solubilities, in particular of the so-called minor species (S-bearing species and
554 halogens), is that they impose limits on absolute quantities of volatile species that a given silicate
555 melt may dissolve. Knowing such a limit allows for the determination of the magma volume
556 implied at depth to sustain gas emissions measured during an eruptive period, either effusive or
557 explosive. This is, however, possible only when there is no excess gas phase (bubble) in the
558 reservoir. Bubbles may indeed store a dominant part of some volatile species (C- and S-bearing):
559 the use of S or C fluxes measured at the surface in terms of magma mass stored at depth would
560 require knowing the amount of bubbles in the reservoir, a quantity notoriously difficult to estimate
561 (e.g., Wallace et al., 1995, Papale, 2005).

562 The determination of volatile solubilities allows also for the calculation of gas composition
563 at equilibrium with the magma either in the reservoir (Scaillet and Pichavant, 2003) or during its
564 upraise toward the surface (Burgisser and Scaillet, 2007). This application offers potentially a
565 powerful tool for the interpretation of volcanic gas compositions measured at the surface in active
566 volcanic areas (Fig. 9b). It is indeed well documented that fluctuations in gas compositions occur
567 prior or during eruptions (e.g., Allard et al., 2005; Burton et al., 2007; Aiuppa et al., 2010;
568 Oppenheimer et al., 2011; Burgisser et al., 2012), but the interpretation in terms of processes still
569 remains elusive. Changes in gas composition with eruptive style are apparent in many cases, yet
570 the real challenge is the detection of precursor gas signals related to unrest phases. A quantitative
571 as well as predictive use of such an approach, requires the modelling of gas-melt equilibria but
572 also gas-melt-crystal equilibria as crystals can hold a significant amount of volatile species
573 (sulfides, sulfates, brines). It also requires integrating the effect of aquifers which can scrub out
574 soluble species from the uprising gas (SO_2 in particular, or HCl), therefore altering the surface

575 signal (Symonds et al., 2001). This field is one of very active research, owing to the many
576 parameters intervening, their coupled character as well as feedback effects (Chiodini et al., 2016).

577 ***Experimental constraints to magma mixing/interaction***

578 As stated previously, it has been long recognized that mixing is a common process occurring
579 in magmatic reservoirs (Sparks et al., 1978). Mixing can take place between magmas differing
580 widely in composition (and rheological properties) or between compositionally similar end-
581 members. Regardless, one of the key-controlling factors of mixing efficiency appears to be the
582 viscosity contrast between juxtaposed magmas, mixing being promoted when both end-members
583 share the same viscosity. Another important parameter is density, particularly when magma
584 blending produces density inversion, since this can lead to chamber-wide convection and eruption.
585 Experiments have tackled mixing using a variety of approaches. Firstly, by juxtaposing magmas
586 with contrasted compositions under static conditions and measuring diffusion exchange at their
587 interface for different run durations (Wyllie et al., 1989). This gives insight into the time scales
588 necessary to generate diffusion profiles sometimes observed in quenched mixtures. Secondly,
589 torsion experiments, done mostly at one bar (i.e. under dry conditions), have allowed to explore
590 the role of shear rate across the interface (e.g., Kouchi and Sunagawa et al., 1985; Campos et al.,
591 2011), showing that high shear rates, such as in volcanic conduits, facilitate mixing, even with
592 high viscosity contrast. The geochemical patterns obtained in such high temperature experiments
593 have been also used to infer the contact time between mixed magmas in volcanic products (e.g.,
594 Perugini et al., 2008; Rossi et al., 2017). More recently, torsion experiments at high pressure (i.e.
595 with hydrous magmas) have demonstrated that mixing between felsic and mafic magmas in
596 reservoirs (i.e., at low strain rates as compared to that in volcanic conduits) occurs only when the
597 viscosity contrast is null (Fig. 10; Laumonier et al., 2014). These experiments provide constraints

598 on the relative amounts between invading and resident magmas needed to achieve homogeneous
599 mixtures at the hand scale (Fig. 11): the experiments and ensuing calculations show that true
600 hybrids require in general equal amounts of mafic and felsic magmas, a too small amount
601 preventing the production of intermediate magmas in any significant volume. At a somewhat
602 smaller scale, experiments have also investigated the rate of diffusive equilibration of crystals
603 exposed to changing P-T or chemical conditions. As stated above, the preservation of chemical
604 zoning in many phenocrysts (olivine, feldspars, pyroxenes, oxides), and their interpretation in
605 terms of relaxation time scale, offer a powerful tool for gauging the residence times of crystals in
606 magmas. This approach most often concludes to relatively short time scales of attending magmatic
607 processes (i.e. magma recharge) occurring before eruption, from hours to months to decades (e.g.,
608 Costa et al., 2003; Druitt et al., 2012).
609 Experiments can also explore how a magma, once intruded in the crust to build a shallow
610 reservoir, interacts with its surroundings. Of particular interest in the context of volcanic processes
611 is the ingestion by the magma of volatile-rich country rocks. Contamination of the magma by
612 evaporites, carbonates or coal-rich sediments has the potential to liberate a variety of S- and C-
613 species which will add to the initial content of those elements of the magma. Recognition of such
614 a process is important since it affects the interpretation of gas fluxes measured at the surface (e.g.,
615 Di Rocco et al., 2012). Whenever this happens, the mass of volatiles expelled cannot be used to
616 make inferences about the amount of the magma source of these emissions, unless isotopic
617 discrimination between magma and host rock volatiles is possible. The contamination process not
618 only affects the volatile budget of the magma but also its redox state which in turn affects gas
619 speciation, with these interactions being progressively able to affect the magma chemical evolution
620 (Iacono-Marziano et al., 2008, 2012). Such an evolution can be in turn correlated to a change of

621 the plumbing system (nature of the host rock with depth). If good inferences can be made about
622 the host rock (generally by looking at xenoliths carried by the magmas), interaction experiments
623 can thus provide important constraints on the plumbing system and the way it affects magma
624 evolution and its surface manifestations (i.e. gas composition). Fluxing of externally generated
625 volatiles through a magma reservoir can also induce important variations in the volatile solubility
626 of the magma, changing the composition (and partial pressure) of the coexisting fluids (Spilliaert
627 et al., 2005; Dallai et al., 2011).

628 ***Constraints to the rates of magma ascent: decompression experiments***

629 This category of experiments is obviously the one more closely simulating magma ascent in
630 a conduit. The fundamental parameter that those experiments strive to constrain is the magma
631 ascent rate and its potential variation during the eruptive sequence. Textural features that
632 experiments aim at replicating are crystal and bubble size distributions. Compositional features are
633 primarily microlite compositions and glass volatile contents. For the latter, the contrasted kinetics
634 of volatile species diffusion afford potentially a powerful speedometer. However, given the
635 difficulty in quantitatively analyzing dissolved volatiles in quenched experimental run products,
636 efforts have focused mostly on reproducing bubble (e.g., Mangan and Sisson, 2000; Mourtada-
637 Bonnefoi and Laporte, 2004; Gardner and Ketcham, 2011; Martel and Iacono-Marziano, 2015; Le
638 Gall and Pichavant, 2016) and microlite (e.g., Hammer et al., 1999; Martel, 2012) characteristics.
639 This category of experiments show that it is possible to simulate accurately the texture of volcanic
640 rocks, giving strong confidence on the reliability of the constrained parameter. Ascent rates
641 inferred from such an approach show that the transit time between magma reservoir and the sub-
642 surface varies from hours to days, depending on eruptive dynamics and magma composition.

643 Decompression experiments have the potential to unravel in considerable detail the
644 behavior of volatiles during magma ascent (e.g., Fiege et al., 2015; Le Gall and Pichavant, 2016).
645 This is important because such a knowledge helps to understand not only the physical effects
646 associated to volatile exsolution (i.e. when bubbles nucleate and how they grow) but also the
647 associated chemical effects: the latter arise because of the differing kinetics of volatile species
648 diffusion in silicate melts (Watson, 1994; Baker et al., 2005), slower diffusing species (CO_2, S-
649 bearing) lagging behind (i.e. remaining within the melt) species with high mobility (H_2O, H_2). This
650 diffusive fractionation of volatile species will in turn affect gas composition, that will necessarily
651 differ from the one which can be calculated under the equilibrium assumption, using known
652 solubility laws (Fig. 12). Essentially, gas produced during fast magma ascent will be richer in H_2O
653 than predicted by equilibrium (Pichavant et al., 2013), though the details of chemical effects
654 associated to decompression still remain largely unexplored. This comparatively new field of
655 research, made possible by the improved performances of laboratory experiments and micro-
656 analytical tools (ion probe or infra-red spectroscopy), will expand in the next coming years.

657 ***Measuring physical properties of rocks and magmas***

658 This is also a rapidly expanding field that aims at defining the physical properties of rocks
659 and magmas under their natural conditions. A master property that has fuelled numerous laboratory
660 studies is magma viscosity. Thanks to a wealth of experimental data, acquired on either dry or
661 hydrous systems, there are now efficient models for calculating melt viscosities under a large range
662 of T-volatiles conditions (e.g., Giordano et al., 2008). The effects of crystals and bubbles (e.g.,
663 Bagdassarov and Dingwell, 1992; Rust and Manga, 2002) have been also extensively explored,
664 these efforts enabling the elaboration of various accurate models of magma rheology (e.g., Costa,
665 2005; Mader et al., 2013). The role of strain rate on magma rheology has been also explored at

high pressure (e.g., Caricchi et al., 2011). These data primarily serve to inform numerical simulations of magma flow (within reservoirs or conduits) whose performances heavily depend on the robustness of the constitutive laws used for describing material properties, and their evolution with intensive parameters (e.g., Costa et al., 2011). The conditions leading to magma or host rock fracture, and the measurement of associated signals, is evidently an important field of research (e.g., Benson et al., 2012; Heap et al., 2015; Vasseur et al., 2018), although still in its infancy owing to the variety of lithologies and conditions involved in nature.

Laboratory experiments also helps to interpret the geophysical signals measured at the surface (seismicity, conductivity, gravimetry, etc.) which are used to image magma bodies beneath volcanoes. Although technically challenging, the attenuation of the velocity of seismic waves with fraction of melt/fluid has been studied at high pressure and high temperature, but the difference in frequency between natural and laboratory waves is a complicating factor for data application (Caricchi et al., 2008). In-situ measurements allow now to measure directly the density of hydrous melts at high pressure (Malfait et al., 2014), which should be of considerable help for interpreting gravimetric anomalies in volcanic areas. Finally, it is now possible to measure with great precision the variation of the electrical conductivity of melts with their composition, including their volatile contents (Gaillard, 2004; Pommier et al., 2010). These data help illuminate the volcanological significance of magnetotelluric signals detected in active volcanic areas (Pommier et al., 2008). As knowledge is gained in the next coming years, the combination of the above data along with joint inversion of surface signals should considerably improve our ability to detect not only magma bodies, even those small, but also the precursor signals associated to magma upraise or recharge associated to unrest phases.

Discussion and Conclusions

In the last few decades, disciplines such as physical volcanology and petrology have moved from qualitative and descriptive approaches towards a more quantitative approach for the understanding of magmatic and volcanic processes. This advancement produced a huge amount of new data on volcanic deposits, mineral and melt components of volcanic rocks, and generated new ideas and perspectives on laboratory experiments and physical models. By merging these data with those produced by other disciplines (e.g. geophysics), new conceptual models on how volcanoes work have arisen and more precise information on the size and internal dynamics of volcanic systems have been obtained. The most important advancements in this framework have been established at volcanoes with persistent activity or with high eruptive frequency, where hypotheses and conceptual models can be continuously elaborated, tested and refined.

A holistic, multidisciplinary view of volcanic systems through the study of their different portions and products is the only way to reach a robust understanding of the large set of processes which control their activity. A real step forward in the general understanding of a volcanic system can only be obtained starting from the detailed, basic knowledge of its structure and deposits derived from volcanological investigations in the field (geological and structural mapping, geochronology, stratigraphy and sedimentology of the deposits), passing through the physical volcanological characterization of products and eruptions, up to the most accurate, refined petrological studies of the main single processes controlling the volcanic system.

Field volcanology studies represent always the main door to the knowledge of a volcanic system. The under consideration of the geological evolution of a volcanic system can in fact result in a strongly biased reconstruction of the complex set of processes governing and modulating its life. Planning of stratigraphic and mapping work should be always implemented when assessing

712 volcanic hazards or defining the spectrum of eruption scenarios at a volcano. Additionally, data
713 already available for the volcanoes of interest should be always critically revised in the light of
714 new views on volcanic activity and products, instead of accepting them uncritically. Studies of on-
715 going activity are generally strongly preferred in order to understand the dynamics of volcanic
716 activity, but the study of the deposits of past eruptions still remains a unique tool to define the
717 range of possible eruption scenarios at a given volcano.

718 Eruptive activity is strictly related to the physico-chemical conditions of the magma driving
719 the eruption. At the same time, the temporal evolution of a magmatic system is strictly controlled
720 by changes in the magma source or in the physical conditions of magma evolution. For these
721 reasons, the petrological characterization of the erupted products and of their temporal variations
722 can provide important data to derive direct indications on the significance of these processes.
723 Based on all this knowledge, experimental petrology can be used to reproduce effectively in the
724 lab the conditions of magma evolution, ascent and eruption to the surface, adding new, quantitative
725 estimations of the main parameters which control all these processes.

726 Hazard assessment and eruption scenario definition for a volcano should be always based on
727 the deep, direct knowledge of the range of parameters which control its activity and evolution, in
728 the view that each volcano is characterized by its own “personality”.

729

730

731 ## References

732 Acocella, V. (2007). Understanding caldera structure and development: An overview of analogue
733 models compared to natural calderas. Earth-Science Reviews, 85(3-4), 125-160.

734 Acocella, V. (2014). Structural control on magmatism along divergent and convergent plate
735 boundaries: Overview, model, problems. Earth-Science Reviews, 136, 226-288.
736 Acocella, V., Porreca, M., Neri, M., Mattei, M., & Funiciello, R. (2006). Fissure eruptions at
737 Mount Vesuvius (Italy): insights on the shallow propagation of dikes at volcanoes.
738 Geology, 34(8), 673-676.
739 Aiuppa, A., Burton, M., Caltabiano, T., Giudice, G., Guerrieri, S., Liuzzo, M., Murè F., &
740 Salerno, G. (2010). Unusually large magmatic CO2 gas emissions prior to a basaltic
741 paroxysm. Geophysical Research Letters, 37(17).
742 Albert, H., Costa, F. & Marti, J. 2015. Timing of Magmatic Processes and Unrest Associated with
743 Mafic Historical Monogenetic Eruptions in Tenerife Island. Journal of Petrology, 56,
744 1945–1966, doi: 10.1093/petrology/egv058.
745 Albert, H., Costa, F. & Marti, J. 2016. Years to weeks of seismic unrest and magmatic intrusions
746 precede monogenetic eruptions. Geology, 44, 211–214, doi: 10.1130/G37239.1.
747 Allard, P., Burton, M., & Muré, F. (2005). Spectroscopic evidence for a lava fountain driven by
748 previously accumulated magmatic gas. Nature, 433(7024), 407.
749 Alletti, M., Burgisser, A., Scaillet, B., & Oppenheimer, C. (2014). Chloride partitioning and
750 solubility in hydrous phonolites from Erebus volcano: A contribution towards a multi-
751 component degassing model. GeoResJ, 3, 27-45.
752 Andersen, D. J., Lindsley, D. H., & Davidson, P. M. (1993). QUILF: A pascal program to assess
753 equilibria among Fe Mg Mn Ti oxides, pyroxenes, olivine, and quartz. Computers
754 & Geosciences, 19(9), 1333-1350.

755 Anderson Jr, A. T., Newman, S., Williams, S. N., Druitt, T. H., Skirius, C., & Stolper, E. (1989).
756 H2O, CO2, CI, and gas in Plinian and ash-flow Bishop rhyolite. Geology, 17(3), 221-
757 225.
758 Andújar, J., Martel, C., Pichavant, M., Samaniego, P., Scaillet, B., & Molina, I. (2017). Structure
759 of the plumbing system at Tungurahua volcano, Ecuador: insights from phase equilibrium
760 experiments on July–August 2006 eruption products. Journal of Petrology, 58(7), 1249-
761 1278.
762 Andújar, J., Scaillet, B., Pichavant, M., & Druitt, T. H. (2015). Differentiation conditions of a
763 basaltic magma from Santorini, and its bearing on the production of andesite in arc
764 settings. Journal of Petrology, 56(4), 765-794.
765 Andújar, J., Scaillet, B., Pichavant, M., & Druitt, T. H. (2016). Generation conditions of dacite
766 and rhyodacite via the crystallization of an andesitic magma. Implications for the
767 plumbing system at Santorini (Greece) and the origin of tholeiitic or calc-alkaline
768 differentiation trends in arc magmas. Journal of Petrology, 57(10), 1887-1920.
769 Armienti, P. 2008. Decryption of Igneous Rock Textures: Crystal Size Distribution Tools. Reviews
770 in Mineralogy and Geochemistry, 69, 623–649, doi: 10.2138/rmg.2008.69.16.
771 Armienti, P., Perinelli, C. & Putirka, K.D. 2013. A New Model to Estimate Deep-level Magma
772 Ascent Rates, with Applications to Mt. Etna (Sicily, Italy). Journal of Petrology, 54, 795–
773 813, doi: 10.1093/petrology/egs085.
774 Asimow, P., Dixon, J. & Langmuir, C. 2004. A hydrous melting and fractionation model for mid-
775 ocean ridge basalts: Application to the Mid-Atlantic Ridge near the Azores. Geochemistry
776 Geophysics Geosystems, 5.

777 Azzaro, R., Branca, S., Gwinner, K., & Coltelli, M. (2012). The volcano-tectonic map of Etna
778 volcano, 1: 100.000 scale: an integrated approach based on a morphotectonic analysis from
779 high-resolution DEM constrained by geologic, active faulting and seismotectonic data.
780 Italian Journal of Geosciences, 131(1), 153-170.
781 Bacon, C. R. (1986). Magmatic inclusions in silicic and intermediate volcanic rocks. Journal of
782 Geophysical Research: Solid Earth, 91(B6), 6091-6112.
783 Bagdassarov, N. S., & Dingwell, D. B. (1992). A rheological investigation of vesicular rhyolite.
784 Journal of volcanology and geothermal research, 50(3), 307-322.
785 Baker, D. R., Freda, C., Brooker, R. A., & Scarlato, P. (2005). Volatile diffusion in silicate melts
786 and its effects on melt inclusions. Annals of Geophysics, 48(4-5).
787 Barberi F, Coltelli M, Frullani A, Rosi, M., Almeida, E. (1995) Chronology and dispersal
788 characteristics of recently (last 5000 years) erupted tephra of Cotopaxi (Ecuador):
789 implications for long-term eruptive forecasting. Journal of Volcanology and Geothermal
790 Research 69:217–239.
791 Barsotti, S., Neri, A., & Scire, J. S. (2008). The VOL-CALPUFF model for atmospheric ash
792 dispersal: 1. Approach and physical formulation. Journal of Geophysical Research: Solid
793 Earth, 113(B3).
794 Benson, P. M., Heap, M. J., Lavallee, Y., Flaws, A., Hess, K. U., Selvadurai, A. P. S., ... &
795 Schillinger, B. (2012). Laboratory simulations of tensile fracture development in a
796 volcanic conduit via cyclic magma pressurisation. Earth and Planetary Science Letters,
797 349, 231-239.

798 Blank, J. G., Stolper, E. M., & Carroll, M. R. (1993). Solubilities of carbon dioxide and water in
799 rhyolitic melt at 850 C and 750 bars. Earth and Planetary Science Letters, 119(1-2), 27-
800 36.
801 Blundy, J., & Cashman, K. (2001). Ascent-driven crystallisation of dacite magmas at Mount St
802 Helens, 1980–1986. Contrib Mineral Petrol 140, 631–650. doi:10.1007/s004100000219
803 Blundy, J., & Cashman, K. (2008). Petrologic reconstruction of magmatic system variables and
804 processes. Reviews in Mineralogy and Geochemistry, 69(1), 179-239.
805 Bonadonna, C., Biass, S., Costa, A. (2015). Physical characterization of explosive volcanic
806 eruptions based on tephra deposits: propagation of uncertainties and sensitivity analysis.
807 Journal of Volcanology and Geothermal Research, 296, 80–100.
808 doi:10.1016/j.jvolgeores.2015.03.009
809 Bonadonna, C., Cioni, R., Costa, A., Druitt, T., Phillips, J., Pioli, L., Andronico, D., Harris, A.,
810 Scollo, S., Bachmann, O.Bagheri, G. (2016). MeMoVolc report on classification and
811 dynamics of volcanic explosive eruptions. Bulletin of Volcanology, 78(11), p.84.
812 Bonadonna, C., Cioni, R., Pistolesi, M., Connor, C., Scollo, S., Pioli, L., & Rosi, M. (2013).
813 Determination of the largest clast sizes of tephra deposits for the characterization of
814 explosive eruptions: a study of the IAVCEI commission on tephra hazard modelling.
815 Bulletin of Volcanology, 75(1), 680.
816 Bonadonna, C., Ernst, G. G. J., & Sparks, R. S. J. (1998). Thickness variations and volume
817 estimates of tephra fall deposits: the importance of particle Reynolds number. Journal of
818 Volcanology and Geothermal Research, 81(3-4), 173-187.
819 Brown, S. K., Crosweller, H. S., Sparks, R. S. J., Cottrell, E., Deligne, N. I., Guerrero, N. O.,
820 Hobbs, L., Kiyosugi, K., Loughlin, S. C., Siebert, L., & Takarada, S. (2014).

821 Characterisation of the Quaternary eruption record: analysis of the Large Magnitude
822 Explosive Volcanic Eruptions (LaMEVE) database. Journal of Applied Volcanology, 3(1),
823 5.
824 Burgisser, A., & Scaillet, B. (2007). Redox evolution of a degassing magma rising to the surface.
825 Nature, 445(7124), 194.
826 Burgisser, A., Alletti, M., & Scaillet, B. (2015). Simulating the behavior of volatiles belonging to
827 the C–O–H–S system in silicate melts under magmatic conditions with the software D-
828 Compress. Computers & Geosciences, 79, 1-14.
829 Burgisser, A., Oppenheimer, C., Alletti, M., Kyle, P. R., Scaillet, B., & Carroll, M. R. (2012).
830 Backward tracking of gas chemistry measurements at Erebus volcano. Geochemistry,
831 Geophysics, Geosystems, 13(11).
832 Burton, M., Allard, P., Muré, F., & La Spina, A. (2007). Magmatic gas composition reveals the
833 source depth of slug-driven Strombolian explosive activity. Science, 317(5835), 227-230.
834 Cadoux, A., Scaillet, B., Druitt, T. H., & Deloule, E. (2014). Magma storage conditions of large
835 Plinian eruptions of Santorini Volcano (Greece). Journal of Petrology, 55(6), 1129-1171.
836 Carey, S., & Sigurdsson, H. (1986). The 1982 eruptions of El Chichón volcano, Mexico (2):
837 Observations and numerical modelling of tephra-fall distribution. Bulletin of Volcanology,
838 48(2-3), 127-141.
839 Carey, S., & Sparks, R. S. J. (1986). Quantitative models of the fallout and dispersal of tephra from
840 volcanic eruption columns. Bulletin of volcanology, 48(2-3), 109-125.
841 Caricchi, L., Burlini, L., & Ulmer, P. (2008). Propagation of P and S-waves in magmas with
842 different crystal contents: Insights into the crystallinity of magmatic reservoirs. Journal of
843 Volcanology and Geothermal Research, 178(4), 740-750.

844 Caricchi, L., Pommier, A., Pistone, M., Castro, J., Burgisser, A., & Perugini, D. (2011). Strain-
845 induced magma degassing: insights from simple-shear experiments on bubble bearing
846 melts. Bulletin of volcanology, 73(9), 1245-1257.
847 Cas, R., & Wright, J. (1987). Volcanic successions modern and ancient: A geological approach to
848 processes, products and successions. Springer Science & Business Media.
849 Cashman, K. & Marsh, B. 1988. Crystal Size distribution in rocks and the kinetics and dynamics
850 of crystallization II. Makaopuhi lava lake. Contributions to Mineralogy and Petrology, 99,
851 401–405.
852 Cashman, K. 1992. Groundmass crystallization of Mount St. Helens dacite, 19880-1986: a tool for
853 interpreting shallow magmatic processes. Contributions to Mineralogy and Petrology, 109,
854 431–449.
855 Cashman, K., & Blundy, J. (2000). Degassing and crystallization of ascending andesite and dacite.
856 Philosophical Transactions: Mathematical, Physical and Engineering Sciences 358, 1487–
857 1513.
858 Cashman, K.V., Sparks, R.S.J. & Blundy, J.D. 2017. Vertically extensive and unstable magmatic
859 systems: A unified view of igneous processes. Science, 355, eaag3055–11, doi:
860 10.1126/science.aag3055.
861 Cembrano, J., & Lara, L. (2009). The link between volcanism and tectonics in the southern
862 volcanic zone of the Chilean Andes: a review. Tectonophysics, 471(1-2), 96-113.
863 Chamberlain, K.J., Morgan, D.J. & Wilson, C.J.N. 2014. Timescales of mixing and mobilisation
864 in the Bishop Tuff magma body: perspectives from diffusion chronometry. Contributions
865 to Mineralogy and Petrology, 168, 563–24, doi: 10.1007/s00410-014-1034-2.

866 Charlier, B.L.A., Morgan, D.J., Wilson, C.J.N., Wooden, J.L., Allan, A.S.R. & Baker, J.A. 2012.
867 Lithium concentration gradients in feldspar and quartz record the final minutes of magma
868 ascent in an explosive supereruption. Earth and Planetary Science Letters, 319-320, 218–
869 227, doi: 10.1016/j.epsl.2011.12.016.
870 Chiodini, G., Paonita, A., Aiuppa, A., Costa, A., Caliro, S., De Martino, P., Acocella, V. and
871 Vandemeulebrouck, J. (2016). Magmas near the critical degassing pressure drive volcanic
872 unrest towards a critical state. Nature communications, 7, 13712.
873 Cioni, R. (1993). Il complesso di Bolsena e il vulcanismo alcalino-potassico del Lazio
874 settentrionale. Ph. D. thesis.
875 Cioni, R. (2000). Volatile content and degassing processes in the AD 79 magma chamber at
876 Vesuvius (Italy). Contributions to Mineralogy and Petrology, 140(1), 40-54.
877 Cioni, R., Bertagnini, A., Santacroce, R., & Andronico, D. (2008). Explosive activity and eruption
878 scenarios at Somma-Vesuvius (Italy): towards a new classification scheme. Journal of
879 Volcanology and Geothermal Research, 178(3), 331-346.
880 Cioni, R., Gurioli, L., Sbrana, A., & Vougioukalakis, G. (2000). Precursory phenomena and
881 destructive events related to the Late Bronze Age Minoan (Thera, Greece) and AD 79
882 (Vesuvius, Italy) Plinian eruptions; inferences from the stratigraphy in the archaeological
883 areas. Geological Society, London, Special Publications, 171(1), 123-141.
884 Cioni, R., Gurioli, L., Sbrana, A., & Vougioukalakis, G. (2000). Precursory phenomena and
885 destructive events related to the Late Bronze Age Minoan (Thera, Greece) and AD 79
886 (Vesuvius, Italy) Plinian eruptions; inferences from the stratigraphy in the archaeological
887 areas. Geological Society, London, Special Publications 171, 123–141.

888 Clemente, B., Scaillet, B., & Pichavant, M. (2004). The solubility of sulphur in hydrous rhyolitic
889 melts. Journal of Petrology, 45(11), 2171-2196.
890 Collins, B. D., & Dunne, T. (1986). Erosion of tephra from the 1980 eruption of Mount St. Helens.
891 Geological Society of America Bulletin, 97(7), 896-905.
892 Collins, S.J., Pyle, D.M. & Maclennan, J. 2009. Melt inclusions track pre-eruption storage and
893 dehydration of magmas at Etna. Geology, 37, 571–574, doi: 10.1130/G30040A.1.
894 Coltelli, M., Del Carlo, P., Pompilio, M. & Vezzoli, L. 2005. Explosive eruption of a picrite: The
895 3930 BP subplinian eruption of Etna volcano (Italy). Geophysical Research Letters, 32, 1–
896 4, doi: 10.1029/2005GL024271.
897 Cooper, K.M., Kent, A.J.R., 2014. nature12991. Nature 506, 480–483. doi:10.1038/nature12991
898 Corsaro, R.A. & Métrich, N. 2016. Chemical heterogeneity of Mt. Etna magmas in the last 15ka.
899 Inferences on their mantle sources. Lithos, 252-253, 123–134, doi:
900 10.1016/j.lithos.2016.02.006.
901 Corsaro, R.A. & Pompilio, M. 2004a. Buoyancy-controlled eruption of magmas at Mt Etna. Terra
902 Nova, 16, 16–22, doi: 10.1046/j.1365-3121.2003.00520.x.
903 Corsaro, R.A. & Pompilio, M. 2004b. Magma dynamics in the shallow plumbing system of Mt.
904 Etna as recorded by compositional variations in volcanics of recent summit activity (1995-
905 1999). Journal of Volcanology and Geothermal Research, 137, 55–71, doi:
906 10.1016/j.jvolgeores.2004.05.008.
907 Corsaro, R.A., Civetta, L., Di Renzo, V. & Miraglia, L. 2009a. Petrology of lavas from the 2004-
908 2005 flank eruption of Mt. Etna, Italy: inferences on the dynamics of magma in the shallow
909 plumbing system. Bulletin of Volcanology, 71, 781–793, doi: 10.1007/s00445-009-0264-
910 z.

911 Corsaro, R.A., Metrich, N., Allard, P., Andronico, D., Miraglia, L. & Fourmentraux, C. 2009b.
912 The 1974 flank eruption of Mount Etna: An archetype for deep dike-fed eruptions at
913 basaltic volcanoes and a milestone in Etna's recent history. Journal of Geophysical
914 Research Solid Earth, 114, –, doi: 10.1029/2008JB006013.
915 Corsaro, R.A., Miraglia, L. & Pompilio, M. 2007. Petrologic evidence of a complex plumbing
916 system feeding the July-August 2001 eruption of Mt. Etna, Sicily, Italy. Bulletin of
917 Volcanology, 69, 401–421, doi: 10.1007/s00445-006-0083-4.
918 Costa, A. (2005). Viscosity of high crystal content melts: dependence on solid fraction.
919 Geophysical Research Letters,
920 Costa, A., Melnik, O., Sparks, R. S. J., & Voight, B. (2007). Control of magma flow in dykes on
921 cyclic lava dome extrusion. Geophysical Research Letters, 34(2).
922 Costa, F., Chakraborty, S., & Dohmen, R. (2003). Diffusion coupling between trace and major
923 elements and a model for calculation of magma residence times using plagioclase.
924 Geochimica et Cosmochimica Acta, 67(12), 2189-2200.
925 Crisp, J. A. (1984). Rates of magma emplacement and volcanic output. Journal of Volcanology
926 and Geothermal Research, 20(3-4), 177-211.
927 D'Oriano, C., Bertagnini, A. & Pompilio, M. 2011. Ash erupted during normal activity at
928 Stromboli (Aeolian Islands, Italy) raises questions on how the feeding system works.
929 Bulletin of Volcanology, 73, 471–477, doi: 10.1007/s00445-010-0425-0.
930 Dallai L, Cioni R, Boschi C, D'Oriano C (2011) Carbonate-derived CO2 purging magma at depth:
931 Influence on the eruptive activity of Somma-Vesuvius, Italy. Earth and Planetary Science
932 Letters 310: 84–95. doi: 10.1016/j.epsl.2011.07.013

933 De Campos, C. P., Perugini, D., Ertel-Ingrisch, W., Dingwell, D. B., & Poli, G. (2011).
934 Enhancement of magma mixing efficiency by chaotic dynamics: an experimental study.
935 Contributions to Mineralogy and Petrology, 161(6), 863-881.
936 Del Carlo, P. & Pompilio, M. 2004. The relationship between volatile content and the eruptive
937 style of basaltic magma: the Etna case. Annals of Geophysics, 47, 1423–1432.
938 Del Moro, S., Di Roberto, A., et al. 2015. Xenopumice erupted on 15 October 2011 offshore of El
939 Hierro (Canary Islands): a subvolcanic snapshot of magmatic, hydrothermal and
940 pyrometamorphic processes. Bulletin of Volcanology, 77, –19, doi: 10.1007/s00445-015-
941 0940-0.
942 Di Renzo, V., Corsaro, R.A., Miraglia, L., Pompilio, M. & Civetta, L. 2018. Long and short-term
943 magma differentiation at Mt. Etna as revealed by Sr-Nd isotopes and geochemical data.
944 Earth Science Reviews, 190, 112–130, doi: 10.1016/j.earscirev.2018.12.008.
945 Di Rocco, T., Freda, C., Gaeta, M., Mollo, S., & Dallai, L. (2012). Magma chambers emplaced in
946 carbonate substrate: petrogenesis of skarn and cumulate rocks and implications for CO2
947 degassing in volcanic areas. Journal of Petrology, 53(11), 2307-2332.
948 Dixon, J. E., Stolper, E. M., & Holloway, J. R. (1995). An experimental study of water and
949 carbon dioxide solubilities in mid-ocean ridge basaltic liquids. Part I: calibration and
950 solubility models. Journal of Petrology, 36(6), 1607-1631.
951 Druitt, T. H., Costa, F., Deloule, E., Dungan, M., & Scaillet, B. (2012). Decadal to monthly
952 timescales of magma transfer and reservoir growth at a caldera volcano. Nature,
953 482(7383), 77.

954 Druitt, T.H., Costa, F., Deloule, E., Dungan, M. & Scaillet, B. 2012. Decadal to monthly timescales
955 of magma transfer and reservoir growth at a caldera volcano. Nature, 482, 77–U97, doi:
956 10.1038/nature10706.
957 Engwell, S.L., Sparks, R.S.J., & Carey, S. (2014). Physical characteristics of tephra layers in the
958 deep sea realm: the Campanian Ignimbrite eruption. Geological Society, London, Special
959 Publications 398, 47–64. doi:10.1144/SP398.7
960 Evans, B. W., Hildreth, W., Bachmann, O., & Scaillet, B. (2016). In defense of magnetite-
961 ilmenite thermometry in the Bishop Tuff and its implication for gradients in silicic
962 magma reservoirs. American Mineralogist, 101(2), 469-482.
963 Eychenne, J., Le Pennec, J. L., Ramon, P., & Yepes, H. (2013). Dynamics of explosive paroxysms
964 at open-vent andesitic systems: high-resolution mass distribution analyses of the 2006
965 Tungurahua fall deposit (Ecuador). Earth and Planetary Science Letters, 361, 343-355.
966 Fiege, A., Vetere, F., Iezzi, G., Simon, A., & Holtz, F. (2015). The roles of decompression rate
967 and volatiles (H2O+ Cl±CO2±S) on crystallization in (trachy-) basaltic magma. Chemical
968 Geology, 411, 310-322.
969 Fisher, R. V., & Schmincke, H. U. (1984). Pyroclastic rocks. Springer Science & Business Media.
970 Francalanci, L., Tommasini, S. & Conticelli, S. 2004. The volcanic activity of Stromboli in the
971 1906–1998 AD period: mineralogical, geochemical and and isotope data relevant to the
972 understanding of the plumbing system. Journal of Volcanology and Geothermal Research.
973 Francalanci, L., Avanzinelli, R., Tommasini, S., Heuman, A., Beccaluva, L. & Bianchini, G. 2007.
974 A west-east geochemical and isotopic traverse along the volcanism of the Aeolian Island
975 arc, southern Tyrrhenian Sea, Italy: Inferences on mantle source processes. Cenozoic
976 volcanism in the Mediterranean area, 235.

977 Fuhrman, M. L., & Lindsley, D. H. (1988). Ternary-feldspar modeling and thermometry.
978 American mineralogist, 73(3-4), 201-215.
979 Fulignati, P., Marianelli, P., Santacroce, R., & Sbrana, A. (2004). Probing the Vesuvius magma
980 chamber–host rock interface through xenoliths. Geological Magazine, 141(4), 417-428.
981 Gaillard, F. (2004). Laboratory measurements of electrical conductivity of hydrous and dry
982 silicic melts under pressure. Earth and Planetary Science Letters, 218(1-2), 215-228.
983 Gardner, J. E., & Ketcham, R. A. (2011). Bubble nucleation in rhyolite and dacite melts:
984 temperature dependence of surface tension. Contributions to Mineralogy and Petrology,
985 162(5), 929-943.
986 Gardner, J. E., Rutherford, M., Carey, S., & Sigurdsson, H. (1995). Experimental constraints on
987 pre-eruptive water contents and changing magma storage prior to explosive eruptions of
988 Mount St Helens volcano. Bulletin of Volcanology, 57(1), 1-17.
989 Gardner, J.E., Rutherford, M., Carey, S., & Sigurdsson, H. (1995). Experimental constraints on
990 pre-eruptive water contents and changing magma storage prior to explosive eruptions of
991 Mount St Helens volcano. Bull Volcanol 57, 1–17.
992 Ghiorso, M. & Sack, R. 1995. Chemical mass transfer in magmatic processes IV. A revised and
993 internally consistent thermodynamic model for the interpolation and extrapolation of
994 liquid-solid equilibria in magmatic systems at elevated temperatures and pressures.
995 Contributions to Mineralogy and Petrology, 119, 197–212.
996 Ghiorso, M. S., & Evans, B. W. (2008). Thermodynamics of rhombohedral oxide solid solutions
997 and a revision of the Fe-Ti two-oxide geothermometer and oxygen-barometer. American
998 Journal of science, 308(9), 957-1039.

999 Ghiorso, M.S. & Gualda, G.A.R. 2015. An H2O–CO2 mixed fluid saturation model compatible
1000 with rhyolite-MELTS. Contributions to Mineralogy and Petrology, 169, 1–30, doi:
1001 10.1007/s00410-015-1141-8.
1002 Giaccio, B., Messina, P., Sposato, A., Voltaggio, M., Zanchetta, G., Galadini, F., Gori, S., &
1003 Santacroce, R. (2009). Tephra layers from Holocene lake sediments of the Sulmona Basin,
1004 central Italy: implications for volcanic activity in Peninsular Italy and tephrostratigraphy
1005 in the central Mediterranean area. Quaternary Science Reviews, 28(25-26), 2710-2733.
1006 Giacomoni, P.P., Coltorti-M, Bryce, J.G., Fahnestock, M.F. & Guitreau, M. 2016. Mt. Etna
1007 plumbing system revealed by combined textural, compositional, and thermobarometric
1008 studies in clinopyroxenes. Contributions to Mineralogy and Petrology, 171, 1–15, doi:
1009 10.1007/s00410-016-1247-7.
1010 Giordano, D., Russell, J. K., & Dingwell, D. B. (2008). Viscosity of magmatic liquids: a model.
1011 Earth and Planetary Science Letters, 271(1-4), 123-134.
1012 Green, D., Schmidt, M. & Hibberson, W. 2004. Island-arc ankaramites: Primitive melts from
1013 fluxed refractory lherzolitic mantle. Journal of Petrology, 45, 391–403.
1014 Groppelli, G., & Viereck-Goette, L. (Eds.). (2010). Stratigraphy and geology of volcanic areas
1015 (Vol. 464). Geological Society of America.
1016 Grove, T., Parman, S., Bowring, S., Price, R. & Baker, M. 2002. The role of an H 2 O-rich fluid
1017 component in the generation of primitive basaltic andesites and andesites from the Mt.
1018 Shasta region, N California. Contributions to Mineralogy and Petrology, 142, 375–396.
1019 Gualda, G.A.R., Ghiorso, M.S., Lemons, R.V. & Carley, T.L. 2012. Rhyolite-MELTS: a Modified
1020 Calibration of MELTS Optimized for Silica-rich, Fluid-bearing Magmatic Systems.
1021 Journal of Petrology, 53, 875–890, doi: 10.1093/petrology/egr080.

1022 Gurioli, L. et alii (2015). MeMoVolc consensual document: a review of cross-disciplinary
1023 approaches to characterizing small explosive magmatic eruptions. Bulletin of Volcanology,
1024 77(6), 49.
1025 Hammer, J. E., Cashman, K. V., Hoblitt, R. P., & Newman, S. (1999). Degassing and microlite
1026 crystallization during pre-climactic events of the 1991 eruption of Mt. Pinatubo,
1027 Philippines. Bulletin of Volcanology, 60(5), 355-380.
1028 Hammer, J.E., Cashman, K.V., & Voight, B. (2000). Magmatic processes revealed by textural and
1029 compositional trends in Merapi dome lavas. Journal of Volcanology and Geothermal
1030 Research 100, 165–192.
1031 Hammer, J.E., Cashman, K.V., Hoblitt, R.P. & Newman, S. 1999. Degassing and microlite
1032 crystallization during pre-climactic events of the 1991 eruption of Mt. Pinatubo,
1033 Philippines. Bulletin of Volcanology, 60, 355–380, doi: 10.1007/s004450050238.
1034 Hammer, J.E., Cashman, K.V., Hoblitt, R.P., & Newman, S. (1999). Degassing and microlite
1035 crystallization during pre-climactic events of the 1991 eruption of Mt. Pinatubo,
1036 Philippines. Bull Volcanol 60, 355–380.
1037 Hawkesworth, C., George, R., Turner, S., Zellmer, G., 2004. Time scales of magmatic processes.
1038 Earth and Planetary Science Letters 218, 1–16. doi:10.1016/S0012-821X(03)00634-4
1039 Heap, M. J., Xu, T., Kushnir, A. R., Kennedy, B. M., & Chen, C. F. (2015). Fracture of magma
1040 containing overpressurised pores. Journal of Volcanology and Geothermal Research, 301,
1041 180-190.
1042 Higgins, M.D. & Roberge, J. 2007. Three magmatic components in the 1973 eruption of Eldfell
1043 volcano, Iceland: Evidence from plagioclase crystal size distribution (CSD) and

geochemistry. Journal of Volcanology and Geothermal Research, 161, 247–260, doi: 10.1016/j.jvolgeores.2006.12.002.

Higgins, M.D. 1996. Magma dynamics beneath Kameni volcano, Thera, Greece, as revealed by crystal size and shape measurements. Journal of Volcanology and Geothermal Research, 70, 37–48, doi: 10.1016/0377-0273(95)00045-3.

Higgins, M.D.. Quantitative Textural Measurements in Igneous and Metamorphic Petrology. Cambridge University Press.

Iacono-Marziano, G., Gaillard, F., & Pichavant, M. (2008). Limestone assimilation by basaltic magmas: an experimental re-assessment and application to Italian volcanoes. Contributions to Mineralogy and Petrology, 155(6), 719-738.

Iacono-Marziano, G., Gaillard, F., Scaillet, B., Polozov, A. G., Marecal, V., Pirre, M., & Arndt, N. T. (2012). Extremely reducing conditions reached during basaltic intrusion in organic matter-bearing sediments. Earth and Planetary Science Letters, 357, 319-326.

Jerram, D.A., Dobson, K.J., Morgan, D.J. & Pankhurst, M.J. 2018. The Petrogenesis of Magmatic Systems: Using Igneous Textures to Understand Magmatic Processes. In: Volcanic and Igneous Plumbing Systems. Elsevier, 191–229. doi: 10.1016/B978-0-12-809749-6.00008-X.

Johnson, M. C., & Rutherford, M. J. (1989). Experimental calibration of the aluminum-in-hornblende geobarometer with application to Long Valley caldera (California) volcanic rocks. Geology, 17(9), 837-841.

Kahl, M., Chakraborty, S., Costa, F. & Pompilio, M. 2011. Dynamic plumbing system beneath volcanoes revealed by kinetic modeling, and the connection to monitoring data: An

example from Mt. Etna. Earth and Planetary Science Letters, 308, 11–22, doi: 10.1016/j.epsl.2011.05.008.

Kahl, M., Chakraborty, S., Costa, F., Pompilio, M., Liuzzo, M. & Viccaro, M. 2013. Compositionally zoned crystals and real-time degassing data reveal changes in magma transfer dynamics during the 2006 summit eruptive episodes of Mt. Etna. Bulletin of Volcanology, 75, 692, doi: 10.1007/s00445-013-0692-7.

Kahl, M., Chakraborty, S., Pompilio, M. & Costa, F. 2015. Constraints on the Nature and Evolution of the Magma Plumbing System of Mt. Etna Volcano (1991–2008) from a Combined Thermodynamic and Kinetic Modelling of the Compositional Record of Minerals. Journal of Petrology, 56, 2025–2068, doi: 10.1093/petrology/egv063.

Kahl, M., Viccaro, M., Ubide, T., Morgan, D.J. & Dingwell, D.B. 2017. A Branched Magma Feeder System during the 1669 Eruption of Mt Etna: Evidence from a Time-integrated Study of Zoned Olivine Phenocryst Populations. Journal of Petrology, 58, 443–472, doi: 10.1093/petrology/egx022.

Kamenetsky, V.S., Pompilio, M., M trich, N., Sobolev, A.V., Kuzmin, D.V. & Thomas, R. 2007. Arrival of extremely volatile-rich high-Mg magmas changes explosivity of Mount Etna. Geology, 35, 255, doi: 10.1130/G23163A.1.

Kent, A. J. (2008). Melt inclusions in basaltic and related volcanic rocks. Reviews in Mineralogy and Geochemistry, 69(1), 273-331.

Kouchi, A., & Sunagawa, I. (1985). A model for mixing basaltic and dacitic magmas as deduced from experimental data. Contributions to Mineralogy and Petrology, 89(1), 17-23.

Landi, P., Corsaro, R., Francalanci, L., Civetta, L., Miraglia, L., Pompilio, M. & Tesoro, R. 2008. Magma dynamics during the 2007 Stromboli eruption (Aeolian Islands, Italy):

1089 Mineralogical, geochemical and isotopic data. Journal of Volcanology and Geothermal
1090 Research.
1091 Landi, P., Francalanci, L., et al. 2006. The December 2002–July 2003 effusive event at Stromboli
1092 volcano, Italy: Insights into the shallow plumbing system by petrochemical studies. Journal
1093 of Volcanology and Geothermal Research, 155, 263–284, doi:
1094 10.1016/j.jvolgeores.2006.03.032.
1095 Laumonier, M., Scaillet, B., Pichavant, M., Champallier, R., Andujar, J., & Arbaret, L. (2014).
1096 On the conditions of magma mixing and its bearing on andesite production in the crust.
1097 Nature communications, 5, 5607.
1098 Le Gall, N., & Pichavant, M. (2016). Experimental simulation of bubble nucleation and magma
1099 ascent in basaltic systems: Implications for Stromboli volcano. American Mineralogist,
1100 101(9), 1967-1985.
1101 Lesne, P., Scaillet, B., & Pichavant, M. (2015). The solubility of sulfur in hydrous basaltic melts.
1102 Chemical Geology, 418, 104-116.
1103 Lesne, P., Scaillet, B., Pichavant, M., Iacono-Marziano, G., & Beny, J. M. (2011). The H 2 O
1104 solubility of alkali basaltic melts: an experimental study. Contributions to Mineralogy
1105 and Petrology, 162(1), 133-151.
1106 Longpré, M.A., Klugel, A., Diehl, A. & Stix, J. 2014. Mixing in mantle magma reservoirs prior to
1107 and during the 2011-2012 eruption at El Hierro, Canary Islands. Geology, doi:
1108 10.1130/G35165.1.
1109 Lowenstern, J. B. (2003). Melt inclusions come of age: volatiles, volcanoes, and Sorby's legacy.
1110 In Developments in Volcanology (Vol. 5, pp. 1-21). Elsevier.

1111 Mader, H. M., Llewellin, E. W., & Mueller, S. P. (2013). The rheology of two-phase magmas: A
1112 review and analysis. Journal of Volcanolog
1113 Mangan, M. 1990. Crystal size distribution systematics and the determination of magma storage
1114 times: the 1959 eruption of Kilauea volcano, Hawaii. Journal of Volcanology and
1115 Geothermal Researches, 44, 295–302.
1116 Mangan, M., & Sisson, T. (2000). Delayed, disequilibrium degassing in rhyolite magma:
1117 decompression experiments and implications for explosive volcanism. Earth and
1118 Planetary Science Letters, 183(3-4), 441-455.
1119 Marsh, B. 1988. Crystal size distribution (CSD) in rocks and kinetics and dynamics of
1120 crystallization. Contributions to Mineralogy and Petrology, 99, 277–291.
1121 Martel, C. (2012). Eruption dynamics inferred from microlite crystallization experiments:
1122 application to Plinian and dome-forming eruptions of Mt. Pelée (Martinique, Lesser
1123 Antilles). Journal of Petrology, 53(4), 699-725.
1124 Martel, C., & Iacono-Marziano, G. (2015). Timescales of bubble coalescence, outgassing, and
1125 foam collapse in decompressed rhyolitic melts. Earth and Planetary Science Letters, 412,
1126 173-185.
1127 Martel, C., Pichavant, M., Bourdier, J. L., Traineau, H., Holtz, F., & Scaillet, B. (1998). Magma
1128 storage conditions and control of eruption regime in silicic volcanoes: experimental
1129 evidence from Mt. Pelée. Earth and Planetary Science Letters, 156(1-2), 89-99.
1130 Marti, J., Castro, A., Rodriguez, C., Costa, F., Carrasquilla, S., Pedreira, R. & Bolos, X. 2013.
1131 Correlation of Magma Evolution and Geophysical Monitoring during the 2011-2012 El
1132 Hierro (Canary Islands) Submarine Eruption. Journal of Petrology, 54, 1349–1373, doi:
1133 10.1093/petrology/egt014.

1134 Martí, J., Groppelli, G., & da Silveira, A. B. (2018). Volcanic stratigraphy: a review. Journal of
1135 Volcanology and Geothermal Research, 357, 68-91.
1136 Mastin, L. G., Guffanti, M., Servranckx, R., Webley, P., Barsotti, S., Dean, K., Durant, A., Ewert,
1137 J. W., Neri, A., Rose, W. I., Schnieder, D., Siebert, L., Stunder, B., Swanson, G., Tupper,
1138 A., Volentik, A., & Schneider, D. (2009). A multidisciplinary effort to assign realistic
1139 source parameters to models of volcanic ash-cloud transport and dispersion during
1140 eruptions. Journal of Volcanology and Geothermal Research, 186(1-2), 10-21.
1141 Matthews, N.E., Smith, V.C., Costa, A., Durant, A.J., Pyle, D.M., & Pearce, J.G. (2012). Ultra-
1142 distal tephra deposits from super-eruptions: Examples from Toba, Indonesia and Taupo
1143 Volcanic Zone, New Zealand. Quaternary International 258:54–79. doi:
1144 10.1016/j.quaint.2011.07.010
1145 Meletlidis, S., Di Roberto, A., et al. 2012. Xenopumices from the 2011–2012 submarine eruption
1146 of El Hierro (Canary Islands, Spain): Constraints on the plumbing system and magma
1147 ascent. Geophysical Research Letters, 39, L17302, doi: 10.1029/2012GL052675.
1148 Meletlidis, S., Di Roberto, A., et al. 2015. New insight into the 2011-2012 unrest and eruption of
1149 El Hierro Island (Canary Islands) based on integrated geophysical, geodetical and
1150 petrological data. Annals of Geophysics, 58, doi: 10.4401/ag-6754.
1151 Métrich, N., & Wallace, P. J. (2008). Volatile abundances in basaltic magmas and their degassing
1152 paths tracked by melt inclusions. Reviews in mineralogy and geochemistry, 69(1), 363-
1153 402.
1154 Metrich, N., Bertagnini, A. & Di Muro, A. 2010. Conditions of Magma Storage, Degassing and
1155 Ascent at Stromboli: New Insights into the Volcano Plumbing System with Inferences on
1156 the Eruptive Dynamics. Journal of Petrology, 51, 603–626, doi: 10.1093/petrology/egp083.

1157 Mollo, S., Giacomoni, P.P., Coltorti-M, Ferlito, C., Iezzi, G. & Scarlato, P. 2015. Reconstruction
1158 of magmatic variables governing recent Etnean eruptions: Constraints from mineral
1159 chemistry and P-T-fO(2)-H2O modeling. Lithos, 212, 311–320, doi:
1160 10.1016/j.lithos.2014.11.020.
1161 Moore, G. (2008). Interpreting H2O and CO2 contents in melt inclusions: constraints from
1162 solubility experiments and modeling. Reviews in Mineralogy and Geochemistry, 69(1),
1163 333-362.
1164 Moretti, R., Papale, P., & Ottonello, G. (2003). A model for the saturation of COHS fluids in
1165 silicate melts. Geological Society, London, Special Publications, 213(1), 81-101.
1166 Morgan, D., Jerram, D., Chertkoff, D., Davidson, J., Pearson, D., Kronz, A. & Nowell, G. 2007a.
1167 Combining CSD and isotopic microanalysis: Magma supply and mixing processes at
1168 Stromboli Volcano, Aeolian Islands, Italy. Earth and Planetary Science Letters, 260, 419–
1169 431.
1170 Morgan, D.J., Jerram, D.A., Chertkoff, D.G., Davidson, J.P., Pearson, D.G., Kronz, A. & Nowell,
1171 G.M. 2007b. Combining CSD and isotopic microanalysis: Magma supply and mixing
1172 processes at Stromboli Volcano, Aeolian Islands, Italy. Earth and Planetary Science
1173 Letters, 260, 419–431, doi: 10.1016/j.epsl.2007.05.037.
1174 Mourtada-Bonnefoi, C. C., & Laporte, D. (2004). Kinetics of bubble nucleation in a rhyolitic
1175 melt: an experimental study of the effect of ascent rate. Earth and Planetary Science
1176 Letters, 218(3-4), 521-537.
1177 Németh, K., & Cronin, S. J. (2007). Syn-and post-eruptive erosion, gully formation, and
1178 morphological evolution of a tephra ring in tropical climate erupted in 1913 in West
1179 Ambrym, Vanuatu. Geomorphology, 86(1-2), 115-130.

1180 Newhall, C. G., & Self, S. (1982). The volcanic explosivity index (VEI) an estimate of explosive
1181 magnitude for historical volcanism. Journal of Geophysical Research: Oceans, 87(C2),
1182 1231-1238.
1183 Newhall, C., & Hoblitt, R. (2002). Constructing event trees for volcanic crises. Bulletin of
1184 Volcanology, 64(1), 3-20.
1185 Newman, S., & Lowenstern, J. B. (2002). VolatileCalc: a silicate melt–H2O–CO2 solution
1186 model written in Visual Basic for excel. Computers & Geosciences, 28(5), 597-604.
1187 Nielsen, R. L., Michael, P. J., & Sours-Page, R. (1998). Chemical and physical indicators of
1188 compromised melt inclusions. Geochimica et Cosmochimica Acta, 62(5), 831-839.
1189 O'Hara, M. & Herzberg, C. 2002. Interpretation of trace element and isotope features of basalts:
1190 Relevance of field relations, petrology, major element data, phase equilibria, and magma
1191 chamber modeling in basalt petrogenesis. 66, 2167–2191.
1192 Oppenheimer, C., Scaillet, B., & Martin, R. S. (2011). Sulfur degassing from volcanoes: source
1193 conditions, surveillance, plume chemistry and earth system impacts. Reviews in
1194 Mineralogy and Geochemistry, 73(1), 363-421.
1195 Pamukcu, A. S., Gualda, G. A., Bégué, F., & Gravley, D. M. (2015). Melt inclusion shapes:
1196 Timekeepers of short-lived giant magma bodies. Geology, 43(11), 947-950.
1197 Papale, P. (2005). Determination of total H2O and CO2 budgets in evolving magmas from melt
1198 inclusion data. Journal of Geophysical Research: Solid Earth, 110(B3).
1199 Papale, P., Moretti, R., & Barbato, D. (2006). The compositional dependence of the saturation
1200 surface of H2O+ CO2 fluids in silicate melts. Chemical Geology, 229(1-3), 78-95.
1201 Parat, F., & Holtz, F. (2005). Sulfur partition coefficient between apatite and rhyolite: the role of
1202 bulk S content. Contributions to Mineralogy and Petrology, 150(6), 643-651.

1203 Peltier, A., Bachèlery, P. & Staudacher, T. 2009. Magma transport and storage at Piton de La
1204 Fournaise (La Réunion) between 1972 and 2007: A review of geophysical and geochemical
1205 data. Journal of Volcanology and Geothermal Research, 184, 93–108, doi:
1206 10.1016/j.jvolgeores.2008.12.008.
1207 Perugini, D., De Campos, C. P., Dingwell, D. B., Petrelli, M., & Poli, G. (2008). Trace element
1208 mobility during magma mixing: preliminary experimental results. Chemical Geology,
1209 256(3-4), 146-157.
1210 Petrone, C.M., Bugatti, G., Braschi, E., Tommasini, S., 2016. Pre-eruptive magmatic processes
1211 re-timed using a non-isothermal approach to magma chamber dynamics. Nature
1212 Communications 7, 12946. doi:10.2138/am-1998-9-1022
1213 Pfeiffer, T., Costa, A., & Macedonio, G. (2005). A model for the numerical simulation of tephra
1214 fall deposits. Journal of Volcanology and Geothermal Research, 140(4), 273-294.
1215 Pichavant, M., Di Carlo, I., Le Gac, Y., Rotolo, S.G. & Scaillet, B. 2009. Experimental Constraints
1216 on the Deep Magma Feeding System at Stromboli Volcano, Italy. Journal of Petrology, 50,
1217 601–624, doi: 10.1093/petrology/egp014.
1218 Pichavant, M., Di Carlo, I., Rotolo, S. G., Scaillet, B., Burgisser, A., Le Gall, N., & Martel, C.
1219 (2013). Generation of CO 2-rich melts during basalt magma ascent and degassing.
1220 Contributions to Mineralogy and Petrology, 166(2), 545-561.
1221 Pichavant, M., Martel, C., Bourdier, J. L., & Scaillet, B. (2002). Physical conditions, structure,
1222 and dynamics of a zoned magma chamber: Mount Pelée (Martinique, Lesser Antilles
1223 Arc). Journal of Geophysical Research: Solid Earth, 107(B5), ECV-1.

1224 Pichavant, M., Mysen, B. & Macdonald, R. 2002. Source and H2O content of high-MgO magmas
1225 in island arc settings: an experimental study of a primitive calc-alkaline basalt from St.
1226 Vincent, Lesser Antilles arc. 66, 2193–2209.
1227 Pichavant, M., Pompilio, M., D oriano, C. & Dicarlo, I. 2011. Petrography, mineralogy and
1228 geochemistry of a primitive pumice from Stromboli: implications for the deep feeding
1229 system. European Journal of Mineralogy, 23, 499–517, doi: 10.1127/0935-
1230 1221/2011/0023-2109.
1231 Pichavant, M., Scaillet, B., Pommier, A., Iacono-Marziano, G., & Cioni, R. (2014). Nature and
1232 evolution of primitive Vesuvius magmas: an experimental study. Journal of Petrology,
1233 55(11), 2281-2310.
1234 Pietruszka, A.J., Heaton, D.E., Marske, J.P. & Garcia, M.O. 2015. Two magma bodies beneath the
1235 summit of Kīlauea Volcano unveiled by isotopically distinct melt deliveries from the
1236 mantle. Earth and Planetary Science Letters, 413, 90–100, doi: 10.1016/j.epsl.2014.12.040.
1237 Pistolesi M, Rosi M, Cioni R, Cashman, K. V., Rossotti, A., Aguilera, E. (2011) Physical
1238 volcanology of the post--twelfth-century activity at Cotopaxi volcano, Ecuador: Behavior
1239 of an andesitic central volcano. Geological Society of America Bulletin 123:1193–1215.
1240 doi: 10.1130/B30301.1
1241 Pistolesi, M., Bertagnini, A., Di Roberto, A., Isaia, R., Vona, A., Cioni, R., & Giordano, G. (2017).
1242 The Baia–Fondi di Baia eruption at Campi Flegrei: Stratigraphy and dynamics of a multi-
1243 stage caldera reactivation event. Bulletin of Volcanology, 79(9), 67.
1244 Pistolesi, M., Cioni, R., Bonadonna, C., Elissondo, M., Baumann, V., Bertagnini, A., Chiari, L.,
1245 Gonzales, R., Rosi, M., & Francalanci, L. (2015). Complex dynamics of small-moderate

volcanic events: the example of the 2011 rhyolitic Cordón Caulle eruption, Chile. Bulletin of Volcanology, 77(1), 3.

Pistolesi, M., Cioni, R., Francalanci, L., Bertagnini, A., D'Oriano, C., Braschi, E., & Höskuldsson, Á. (2016). The onset of an eruption: selective assimilation of hydrothermal minerals during pre-eruptive magma ascent of the 2010 summit eruption of Eyjafjallajökull volcano, Iceland. Journal of Volcanology and Geothermal Research 327, 449–458. doi:10.1016/j.jvolgeores.2016.09.011

Pommier, A., Gaillard, F., Malki, M., & Pichavant, M. (2010). Methodological re-evaluation of the electrical conductivity of silicate melts. American Mineralogist, 95(2-3), 284-291.

Pommier, A., Gaillard, F., Pichavant, M., & Scaillet, B. (2008). Laboratory measurements of electrical conductivities of hydrous and dry Mount Vesuvius melts under pressure. Journal of Geophysical Research: Solid Earth, 113(B5).

Pompilio, M., Bertagnini, A. & Métrich, N. 2011. Geochemical heterogeneities and dynamics of magmas within the plumbing system of a persistently active volcano: evidence from Stromboli. Bulletin of Volcanology, 74, 881–894, doi: 10.1007/s00445-011-0571-z.

Pompilio, M., Bertagnini, A., del Carlo, P. & Di Roberto, A. 2017. Magma dynamics within a basaltic conduit revealed by textural and compositional features of erupted ash: the December 2015 Mt. Etna paroxysms. Scientific Reports, 7, 10, doi: 10.1038/s41598-017-05065-x.

Proussevitch, A., Sahagian, D. & Carlson, W. 2007. Statistical analysis of bubble and crystal size distributions: Application to Colorado Plateau basalts. Journal of Volcanology and Geothermal Research, 164, 112–126.

1268 Putirka, K. (2016). Amphibole thermometers and barometers for igneous systems and some
1269 implications for eruption mechanisms of felsic magmas at arc volcanoes. American
1270 Mineralogist, 101(4), 841-858.
1271 Putirka, K. 1997. Magma transport at Hawaii: Inferences based on igneous thermobarometry.
1272 Geology, 25, 69–72.
1273 Pyle, D. M. (2015). Sizes of volcanic eruptions. In The encyclopedia of volcanoes (pp. 257-264).
1274 Academic Press.
1275 Pyle, D.M., Ricketts, G.D., Margari, V., van Andel, T.H., Sinitsyn, A.A., Praslov, N.D., &
1276 Lisitsyn, S. (2006). Wide dispersal and deposition of distal tephra during the Pleistocene
1277 "Campanian Ignimbrite/Y5" eruption, Italy. Quaternary Science Reviews 25, 2713–2728.
1278 doi:10.1016/j.quascirev.2006.06.008
1279 Ridolfi, F., Renzulli, A., & Puerini, M. (2010). Stability and chemical equilibrium of amphibole
1280 in calc-alkaline magmas: an overview, new thermobarometric formulations and
1281 application to subduction-related volcanoes. Contributions to Mineralogy and Petrology,
1282 160(1), 45-66.
1283 Roedder, E. (1979). Origin and significance of magmatic inclusions. Bulletin de Mineralogie,
1284 102(5), 487-510.
1285 Rossi, S., Petrelli, M., Morgavi, D., González-García, D., Fischer, L. A., Vetere, F., & Perugini,
1286 D. (2017). Exponential decay of concentration variance during magma mixing:
1287 Robustness of a volcanic chronometer and implications for the homogenization of
1288 chemical heterogeneities in magmatic systems. Lithos, 286, 396-407.
1289 Rutherford, M. J. (2008). Magma ascent rates. Reviews in Mineralogy and Geochemistry, 69(1),
1290 241-271.

1291 Rutherford, M. J., Sigurdsson, H., Carey, S., & Davis, A. (1985). The May 18, 1980, eruption of
1292 Mount St. Helens: 1. Melt composition and experimental phase equilibria. Journal of
1293 Geophysical Research: Solid Earth, 90(B4), 2929-2947.
1294 Salisbury, M.J., Bohrson, W.A., Clynne, M.A., Ramos, F.C. & Hoskin, P. 2008. Multiple
1295 Plagioclase Crystal Populations Identified by Crystal Size Distribution and in situ
1296 Chemical Data: Implications for Timescales of Magma Chamber Processes Associated
1297 with the 1915 Eruption of Lassen Peak, CA. Journal of Petrology, 49, 1755–1780, doi:
1298 10.1093/petrology/egn045.
1299 Santacroce, R., Cioni, R., Marianelli, P., Sbrana, A., Sulpizio, R., Zanchetta, G., Donahue, D. J.,
1300 & Joron, J. L. (2008). Age and whole rock–glass compositions of proximal pyroclastics
1301 from the major explosive eruptions of Somma-Vesuvius: A review as a tool for distal
1302 tephrostratigraphy. Journal of Volcanology and Geothermal Research, 177(1), 1-18.
1303 Saunders, K., Blundy, J., Dohmen, R. & Cashman, K. 2012. Linking Petrology and Seismology at
1304 an Active Volcano. Science, 336, 1023–1027, doi: 10.1126/science.1220066.
1305 Scaillet, B., & Evans, B. W. (1999). The 15 June 1991 eruption of Mount Pinatubo. I. Phase
1306 equilibria and pre-eruption P–T–f O2–f H2O conditions of the dacite magma. Journal of
1307 Petrology, 40(3), 381-411.
1308 Scaillet, B., & Pichavant, M. (2003). Experimental constraints on volatile abundances in arc
1309 magmas and their implications for degassing processes. Geological Society, London,
1310 Special Publications, 213(1), 23-52.
1311 Scaillet, B., Pichavant, M., & Cioni, R. (2008). Upward migration of Vesuvius magma chamber
1312 over the past 20,000 years. Nature, 455(7210), 216

1313 Scandone, R., Cashman, K.V. & Malone, S.D. 2007. Magma supply, magma ascent and the style
1314 of volcanic eruptions. Earth and Planetary Science Letters, 253, 513–529, doi:
1315 10.1016/j.epsl.2006.11.016.
1316 Schiano, P. 2003. Primitive mantle magmas recorded as silicate melt inclusions in igneous
1317 minerals. Earth Science Reviews, 63, 121–144, doi: 10.1016/S0012-8252(03)00034-5.
1318 Schiavi, F., Kobayashi, K., Moriguti, T., Nakamura, E., Pompilio, M., Tiepolo, M. & Vannucci,
1319 R. 2010. Degassing, crystallization and eruption dynamics at Stromboli: trace element and
1320 lithium isotopic evidence from 2003 ashes. Contributions to Mineralogy and Petrology,
1321 159, 541–561.
1322 Schiavi, F., Tiepolo, M., Pompilio, M. & Vannucci, R. 2006. Tracking magma dynamics by Laser
1323 Ablation (LA)-ICPMS trace element analysis of glass in volcanic ash: the 1995 activity of
1324 Mt. Etna. Geophysical Research Letters, 33, 10.1029/2005GL024789.
1325 Schuth, S., Rohrbach, A., Munker, C., Ballhaus, C., Garbe-Schonberg, D. & Qopoto, C. 2004.
1326 Geochemical constraints on the petrogenesis of arc picrites and basalts, New Georgia
1327 Group, Solomon Islands. Contributions to Mineralogy and Petrology, 148, 288–304.
1328 Shishkina, T. A., Botcharnikov, R. E., Holtz, F., Almeev, R. R., Jazwa, A. M., & Jakubiak, A. A.
1329 (2014). Compositional and pressure effects on the solubility of H2O and CO2 in mafic
1330 melts. Chemical Geology, 388, 112-129.
1331 Simkin, T., Siebert, L., McClelland, L., Bridge, D., Newhall, C. and Latter, J.H., 1981. Volcanoes
1332 of the world: a regional directory, gazetteer, and chronology of volcanism during the last
1333 10,000 years. US Hutchinson Ross Publishing.

1334 Smith, D. & Leeman, W. 2005. Chromian spinel–olivine phase chemistry and the origin of
1335 primitive basalts of the southern Washington Cascades. Journal of Volcanology and
1336 Geothermal Research, 140, 49–66.
1337 Sparks, S. R., Sigurdsson, H., & Wilson, L. (1977). Magma mixing: a mechanism for triggering
1338 acid explosive eruptions. Nature, 267(5609), 315.
1339 Spilliaert N, Allard P, Metrich N, Sobolev AV (2006) Melt inclusion record of the conditions of
1340 ascent, degassing, and extrusion of volatile-rich alkali basalt during the powerful 2002
1341 flank eruption of Mount Etna (Italy). J Geophys Res 111:B04203. doi:
1342 10.1029/2005JB003934
1343 Streck, M.J., Leeman, W.P. & Chesley, J. 2007. High-magnesian andesite from Mount Shasta: A
1344 product of magma mixing and contamination, not a primitive mantle melt. Geology, 35,
1345 351, doi: 10.1130/G23286A.1.
1346 Sulpizio, R., Cioni, R., Di Vito, M.A., Mele, D., Bonasia, R., & Dellino, P. (2010). The Pomici di
1347 Avellino eruption of Somma-Vesuvius (3.9 ka bp). Part I: stratigraphy, compositional
1348 variability and eruptive dynamics. Bull Volcanol 72, 539–558. doi:10.1007/s00445-009-
1349 0339-x
1350 Symonds, R. B., Gerlach, T. M., & Reed, M. H. (2001). Magmatic gas scrubbing: implications
1351 for volcano monitoring. Journal of Volcanology and Geothermal Research, 108(1-4),
1352 303-341.
1353 Taddeucci, J., Pompilio, M. & Scarlato, P. 2004. Conduit processes during the July–August 2001
1354 explosive activity of Mt. Etna (Italy): inferences from glass chemistry and crystal size
1355 distribution of ash particles. Journal of Volcanology and Geothermal Research, 137, 33–
1356 54.

1357 Thordarson et al. 2009
1358 Thouret, J. C. (1999). Volcanic geomorphology—an overview. Earth-science reviews, 47(1-2),
1359 95-131.
1360 Tibaldi, A., Corazzato, C., Apuani, T., & Cancelli, A. (2003). Deformation at Stromboli volcano
1361 (Italy) revealed by rock mechanics and structural geology. Tectonophysics, 361(3-4), 187-
1362 204.
1363 Todde, A., Cioni, R., Pistolesi, M., Geshi, N., & Bonadonna, C. (2017). The 1914 Taisho eruption
1364 of Sakurajima volcano: stratigraphy and dynamics of the largest explosive event in
1365 Japanduring the twentieth century 1–22. doi:10.1007/s00445-017-1154-4
1366 Tomiya-A & Takahashi, E. 1995. Reconstruction of an Evolving Magma Chamber beneath Usu
1367 Volcano since the 1663 Eruption. Journal of Petrology, 36, 617–636, doi:
1368 10.1093/petrology/36.3.617.
1369 Tommasini, S., Avanzinelli, R. & Francalanci, L. 2007. The fate of high-angle dipping slabs in the
1370 subduction factory: An integrated trace element and radiogenic isotope (U, Th, Sr, Nd, Pb)
1371 study of Stromboli volcano, Aeolian Arc, Italy. Journal of Petrology, 48, 2407–2430.
1372 Tonarini, S., Armienti, P., D'Orazio, M. & Innocenti, F. 2001. Subduction-like fluids in the genesis
1373 of Mt. Etna magmas: evidence from boron isotopes and fluid mobile elements. Earth and
1374 Planetary Science Letters, 192, 471–483.
1375 Troll, V.R., Klugel, A., et al. 2012. Floating stones off El Hierro, Canary Islands: xenoliths of pre-
1376 island sedimentary origin in the early products of the October 2011 eruption. Solid Earth,
1377 3, 97–110, doi: 10.5194/se-3-97-2012.
1378 Ubide, T. & Kamber, B.S. 2018. Volcanic crystals as time capsules of eruption history. Nature
1379 Communications, 9, 1–12, doi: 10.1038/s41467-017-02274-w.

Vasseur, J., Wadsworth, F. B., & Dingwell, D. B. (2018). Predicting multiphase magma failure at the laboratory scale using acoustic emission data. Frontiers in Earth Science, 6, 132.

Vetere, F., Botcharnikov, R. E., Holtz, F., Behrens, H., & De Rosa, R. (2011). Solubility of H2O and CO2 in shoshonitic melts at 1250 C and pressures from 50 to 400 MPa: implications for Campi Flegrei magmatic systems. Journal of Volcanology and Geothermal Research, 202(3-4), 251-261.

Wallace, P. J., Anderson Jr, A. T., & Davis, A. M. (1995). Quantification of pre-eruptive exsolved gas contents in silicic magmas. Nature, 377(6550), 612.

Waters, L. E., & Lange, R. A. (2015). An updated calibration of the plagioclase-liquid hygrometer-thermometer applicable to basalts through rhyolites. American Mineralogist, 100(10), 2172-2184.

Watson, E. B. (1994). Diffusion in volatile-bearing magmas. Reviews in Mineralogy and Geochemistry, 30(1), 371-411.

Webster, J. D., & Piccoli, P. M. (2015). Magmatic apatite: A powerful, yet deceptive, mineral. Elements, 11(3), 177-182.

Wilson, B. M. (2007). Igneous petrogenesis a global tectonic approach. Springer Science & Business Media.

Wright, T.L. & Klein, F.W. 2006. Deep magma transport at Kilauea volcano, Hawaii. Lithos, 87, 50–79, doi: 10.1016/j.lithos.2005.05.004.

Wyllie, P. J., Carroll, M. R., Johnston, A. D., Rutter, M. J., Sekine, T., & Van der Laan, S. R. (1989). Interactions among magmas and rocks in subduction zone regions: experimental studies from slab to mantle to crust. European Journal of Mineralogy, 1(2), 165-179.

1402 Zellmer, G.F., Blake, S., Vance, D., Hawkesworth, C. & Turner, S. 1999. Plagioclase residence
1403 times at two island arc volcanoes (Kameni Islands, Santorini, and Soufriere, St. Vincent)
1404 determined by Sr diffusion systematics. Contributions to Mineralogy and Petrology, 136,
1405 345–357, doi: 10.1007/s004100050543.
1406 Zellmer, G.F., Sparks, R.S.J., Hawkesworth, C.J. & Wiedenbeck, M. 2003. Magma Emplacement
1407 and Remobilization Timescales Beneath Montserrat: Insights from Sr and Ba Zonation in
1408 Plagioclase Phenocrysts. Journal of Petrology, 44, 1413–1431, doi:
1409 10.1093/petrology/44.8.1413.
1410 Zieg, M. & Marsh, B. 2002. Crystal size distributions and scaling laws in the quantification of
1411 igneous textures. Journal of Petrology, 43, 85–101.
1412

1413 ## Figure captions

1414 Fig. 1 Idealized view of a magmatic system of a volcano. Right side shows the main
1415 methodologies usually employed for the study of the different portions of the plumbing system
1416 and associated limits (dotted line).
1417

1418 Fig. 2 Reconstructing the stratigraphy of the deposits at the scale of an entire volcanic
1419 edifice is a basilar step to understand the evolution of that volcano and to start a detailed mapping
1420 of the area. A) On the southern sector of Cotopaxi volcano, the main steep gullies (barrancas) show
1421 the whole stratigraphic sequence of deposits emplaced during the last 5 ka consisting of an
1422 alternation of tephra and lava deposits. B) The merging of multiple sections, on the other hand,
1423 allowed a detailed reconstruction of the last 800 years of activity at Cotopaxi (Pistolesi et al.,
1424 2011). A synthetic stratigraphic log highlights the complexity and the large variability of the

1425 eruptive dynamics which led to the emplacement of lapilli and ash layers intercalated to scoria-
1426 flow deposits.
1427
1428 Fig. 3 In order to reconstruct the compositional variability of the erupted products, it is
1429 always important to discuss both the variability at the scale of a single eruption (or eruptive cycle)
1430 and the time-related changes in magma composition. The last 22 ka of activity at Somma-Vesuvius
1431 show a clear trend of increasing alkalinity with time, and large compositional variability of the
1432 magma erupted during single eruptions or during short eruptive cycles. The data can be discussed
1433 in terms of source-related changes in the magma feeding the shallow reservoirs, and of different
1434 processes and physico-chemical conditions of crystallization, refilling and assimilation/fluid
1435 exchange in these reservoirs (data from Santacroce et al., 2008).
1436
1437 Fig. 4 Detailed geochronological reconstructions of the activity of a volcano reveal the
1438 temporal trends of volcanic activity and are important to define the expected time scale for volcanic
1439 reactivation. A) The schematic chronogram of Cotopaxi activity during the last 2000 yr B.P.
1440 clearly shows the presence of eruption clusters (with no obvious intervening soils) separated by
1441 long periods during which only a few large eruptions occur (Barberi et al., 1995; Pistolesi et al.,
1442 2011). These two contrasting behaviors of the volcano over the past 2000 yrs were also observed
1443 in the eruption pattern of the past 800 yrs of activity. During the period A.D. 1150–1742, the
1444 average magma eruption rate was low, and activity consisted of isolated explosive eruptions, while
1445 during the period A.D. 1742–1880, the average magma eruption rate was higher, and activity was
1446 dominated by numerous explosive events separated by eruptive pauses that lasted from a few years
1447 to a few decades (eruption cluster). The eighteenth- to nineteenth-century cluster started with

1448 Plinian outbursts (A.D. 1742–1744), followed by very high intensity and magnitude Plinian bursts
1449 (A.D. 1766–1768). These large events were eventually followed by a period of long-lasting,
1450 moderate-intensity magma degassing mixed with staggered, low- intensity and low-magnitude
1451 explosive bursts, each dominated by a short-lived sub Plinian/violent Strombolian phase followed
1452 by boiling-over activity and associated scoria flows. B). The chronogram of the last 22 ka of
1453 activity Mt. Somma-Vesuvius volcano shows a different behavior with respect to Cotopaxi.
1454 Activity is characterized by a number of large eruptions (Plinian and subplinian) separated by
1455 repose times whose duration varies with age. In fact, while the activity between 22 and 4 ka ago
1456 was mainly characterized by episodic events of large intensity (and magnitude; Cioni et al., 2008)
1457 separated by progressively decreasing repose times, in the last 4000 years the activity became more
1458 and more frequent. The increase in frequency of the eruptions coincided with a general decrease
1459 of their intensity (and magnitude). These changes are clearly associated with changes in magma
1460 composition. Accurate geological reconstructions suggest that the observed lower frequency in the
1461 oldest activity is real and not related to an incomplete geological record, although the problem of
1462 incompleteness in the geological record should always be discussed in detail.
1463
1464 Fig. 5 The detailed, multiparametric reconstruction of a complex eruptive sequence is the
1465 key to the definition of the main eruptive processes which controlled past eruption, and can be
1466 used to define the range of eruption scenarios characterizing a given volcano. The Baia–Fondi di
1467 Baia eruption (9525–9696 BP) is one of the sporadic events that have occurred in the western
1468 sector of the Campi Flegrei caldera and opened Epoch 2 of the caldera activity after a 1000-year-
1469 long period of quiescence. Although relatively small in terms of erupted volume with respect to
1470 most of the events of the past 15 ka, the Baia–Fondi di Baia eruption was characterized by a

1471 complex series of events, which were reconstructed based on a detailed stratigraphic study
1472 (Pistolesi et al., 2017). The idealized composite stratigraphy of the different phases of the eruption
1473 shows how sedimentological data (grains-size and componentry) concur in identifying different
1474 eruptive locations and emplacement dynamics (on-land vs. shallow water vent, fall-out vs. PDC
1475 deposits). Bulk density (gcm^{-3}), vesicularity (vol.%), Vesicle Number Density (cm^{-3}), and
1476 decompression rate ($MPas^{-1}$) data linked to variations in SiO_2, CaO, and K_2O (wt.%) contents
1477 further indicate different types of juvenile material (e.g. variable conditions during ascent in the
1478 conduit) as well as variable magma sources involved in the eruption.
1479
1480 Fig. 6 Simplified interpretative model of the plumbing system of Stromboli (modified by
1481 Métrich et al, 2011) based on (1) the melt compositions and melt saturation pressures recorded by
1482 sealed melt inclusions and unsealed embayments trapped during olivine crystallization, (2) the
1483 crystal textures and (3) the chemistry of Stromboli pumice and scoria samples. LP and HP refer to
1484 low- and high-porphyritic magmas, respectively, according to Francalanci et al. (2004).
1485
1486 Fig. 7 (a) Example of a simplified system analysis of the zoning patterns recorded in olivine
1487 crystals of 1991-1993 Etna eruption. Each box represents a magmatic reservoir of different
1488 composition identified by the overall core plateau compositions and zoning patterns. M0, M1 and
1489 M2 represent end member reservoirs whereas mm1 is a reservoir of mixing. The colored lines
1490 represent the zoning patterns recorded in single olivine crystals. The arrows indicate the direction
1491 of the zonings from core to rim (see details in the original paper). (b) Information distilled from
1492 (a) to highlight the three main magma pathways M0–M1–mm1 (light gray bar) M1–mm1 (dark
1493 gray bar) and M2– mm1 (black bar). (c) An example of a physical plumbing system that is

consistent with (a) and (b). Black dotted lines mark the preferred path followed by many crystals. Various timescales (Δt1, Δt2 and Δt3) that can be extracted from kinetic modeling relate to duration of residence of melts in different segments of the plumbing system, as shown here. From Kahl et al. (2011).

Fig. 8 Phase equilibria of Vesuvius phonolites (Scaillet et al., 2008) showing pre-eruptive conditions inferred for the AD 79 Pompei and AD 472 Pollena events. The top panels show the isobaric-polythermal phase relationships at 200 MPa (2 kbar) for the two compositions as a function of temperature and fluid composition, here expressed as the mole fraction of water ($XH_2Ofluid$). The bottom panels show the polybaric-isothermal sections as a function also of $XH_2Ofluid$. For the isobaric sections, the correspondence with dissolved melt water content (H_2Omelt) is given on the horizontal axis. All sections have been established at an fO_2 one log unit above the Ni-NiO transition (NNO+1). Black squares represent experimental charges. The stability fields of the main phases are labelled with mineral acronyms lying inside the corresponding stability field. The dashed line represents the volume proportion of crystals at 10%. The infered pre-eruptive conditions are indicated by the red filled box and corresponds to the T-$XH_2Ofluid$ locus where the phenocryst assemblage observed in the pumices is experimentally reproduced. The green rectangle gives the melt water content inferred from the analyses of melt inclusions in phenocrysts (Cioni, 2000). For the Pompeii eruption, it is possible to reproduce the phenocrysts proportion and assemblage at 200 MPa, whereas for the Pollena event this is possible only at 100 MPa. This shows that the level of magma accumulation beneath Vesuvius shifted from 200 MPa up to 100 MPa, or about 3 km depth less, in less than 400 years. Acronyms for phases are as

follows: Feld: feldspar, Leuc: leucite; Scap: scapolite; Neph: nepheline; Cpx: clinopyroxene; Gt: garnet; Amph: amphibole, Sod: sodalite.

Fig. 9. a) The contrasted solubilities of H_2O and CO_2 in shoshonite melts from Campi Flegrei volcano (Vetere et al. 2011). The solid lines represent isobars. The dashed lines are isopleths of constant fluid composition for the melts saturated with H_2O–CO_2-bearing flluids. The various symbols indicate the pressure (in MPa) at which the solubility experiments (symbols with attached errors) were done with either pure H_2O (horizontal axis) or mixed H_2O–CO_2 fluids. Note the contrasted solubilities of water (wt%) and CO_2 (ppm). b) Simulation of gas composition during the ascent of a rhyolitic magma (Burgisser and Scaillet, 2007). This type of simulation uses the solubility laws for the volatile species present in the system, in the example shown H_2O, H_2, SO_2, H_2S, S_2. The simulations show the variation of H_2S/SO_2 ratio in the gas phase of an ascending rhyolitic magmas (initially lying at 2000 bar) for various starting conditions in terms of redox state (here expressed as dNNO) and amount of fluid phase initially presents in the reservoir. The vertical black rectangle indicates the measured H_2O/SO_2 ratio of actual volcanic gases at silicic volcanoes, showing that the simulation broadly captures the first order chemical patterns expressed by volcanic gases.

Fig. 10 Image of experimentally mixed magmas under either dry or hydrous conditions (Laumonier et al., 2014). All experiments were performed at 300 MPa but at different temperatures depending on the dry or hydrous character of the system, as indicated on the figure. In both dry and hydrous conditions, the transition between no mixing (left panels) and onset of mixing (right panels) occurs over a very short temperature interval (about 10-15°C) and is related to the slight

change in crystal proportion that controls the viscosity of the mafic end-member (basalt composition, always lying at the bottom). The overlying felsic end member is a crystal-free dacite melt. Note that prior to the onset of mixing the boundary between the two end-members remains sharp and straight, while when mixing starts a crenulate interface develops with production of enclaves (right down panel) that may in turn disaggregate as deformation proceeds (top right panel). For each run, the amount of finite deformation applied to the sample is given (γ). Run durations are on the order of a few hours each.

Fig. 11 The conditions favoring magma mixing at 200 MPa. The different panels show the evolution of the viscosities of the mafic-felsic magmas being juxtaposed depending on fraction of mafic magma injected into the felsic reservoir (Laumonier et al., 2014). The starting temperature of each magma is given (figures color-coded with viscosity trends). Felsic magmas are all water saturated while the basalt may be either dry (1145°C) or H_2O-saturated (980°C). In each panel, optimum mixing conditions are reached when the two viscosity curves cross-over. The vertical thick grey lines give the proportion of the mafic magma needed to achieve conditions favorable to mixing as well as the temperature of the homogeneous mixture so produced. The SiO2 content of that mixture is given on the horizontal top axis of each panel. Numbers labelling each curves give the crystal fraction in each end-member (the r parameter is the average axial ratio of crystals, which controls the bulk viscosity, see Laumonier et al. (2014)). In every case, the proportion of crystals increases in the mafic component, while it decreases in the felsic one, the latter ending almost always crystal-free by the time mixing is possible (vertical grey lines). For instance, the production of a homogeneous andesitic magma by mixing a hydrous basalt at 980°C with a rhyolite at 780°C (panel F), requires the injection of 76 wt% basalt into the rhyolitic reservoir. This ends-up

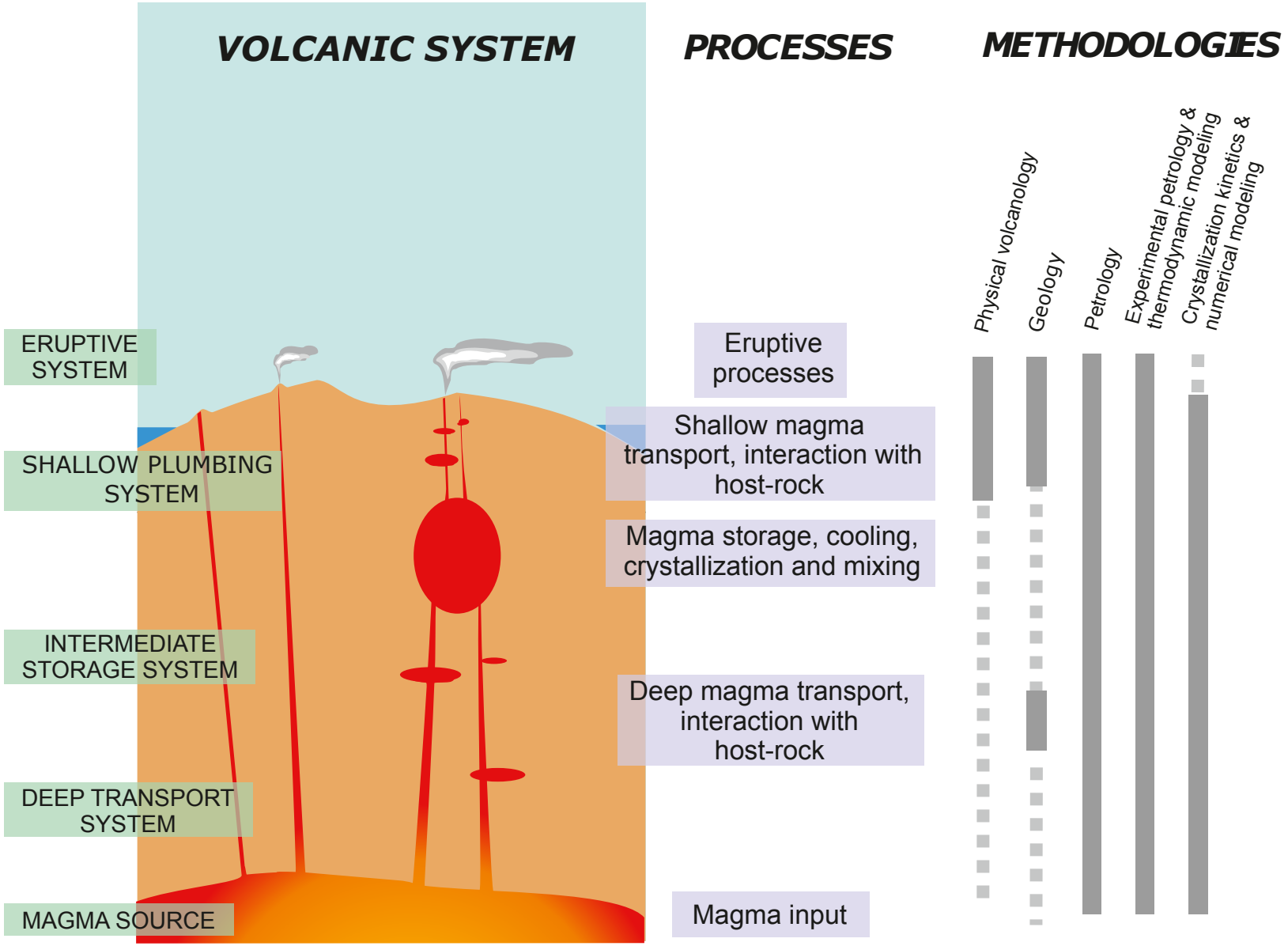
1562 producing an andesite mixture with 57 wt% SiO_2 at a temperature of 934°C. In general, when the
1563 composition of two end-members mixed strongly differ from each other (ie basalt with rhyolite),
1564 the proportion of mafic magma is about 70 wt% (to achieve equal viscosities).
1565
1566 Fig. 12 The effect of decompression on the volatile contents of silicate melts. The figure
1567 shows the measured H_2O and CO_2 contents of basaltic glasses (using a basalt from Stromboli as
1568 starting material) obtained in decompression experiments simulating magma ascent at Stromboli
1569 (Pichavant et al., 2013). The circles represent the starting conditions of each experiment in terms
1570 of volatile content. The oblique thin continuous lines are the isobaric H_2O-CO_2 contents, calculated
1571 using the model of Papale et al. (2006). Squares show the volatile contents of glasses measured
1572 after decompression and quenching at a final pressure of 45-50 MPa at different ascent rates (0.25
1573 to 1.5 m/s). Losange symbols are experiments quenched at 25 MPa final pressure. The
1574 correspondence between starting and final conditions is color coded (i.e. grey circles correspond
1575 to grey squares). The arrowed thin dashed lines are the equilibrium melt volatile contents
1576 calculated for each starting composition, using Papale et al. (2006)'s model. Such calculated paths
1577 are typically near vertical for the high-pressure part of the decompression interval, reflecting the
1578 preferential loss of CO_2, owing to its much lower solubility compared to H_2O, the latter remaining
1579 dissolved for the most part. It is only close to the surface that H_2O is lost. The experiments show,
1580 however, that in out-of equilibrium experiments, quenched glasses preserve a high pressure
1581 signature of CO_2, whose intensity depends on the ascent rate. Supersaturation in CO_2 arising from
1582 decompression may thus give rise to patterns resembling those produced by CO_2-gas fluxing at
1583 depth.
1584

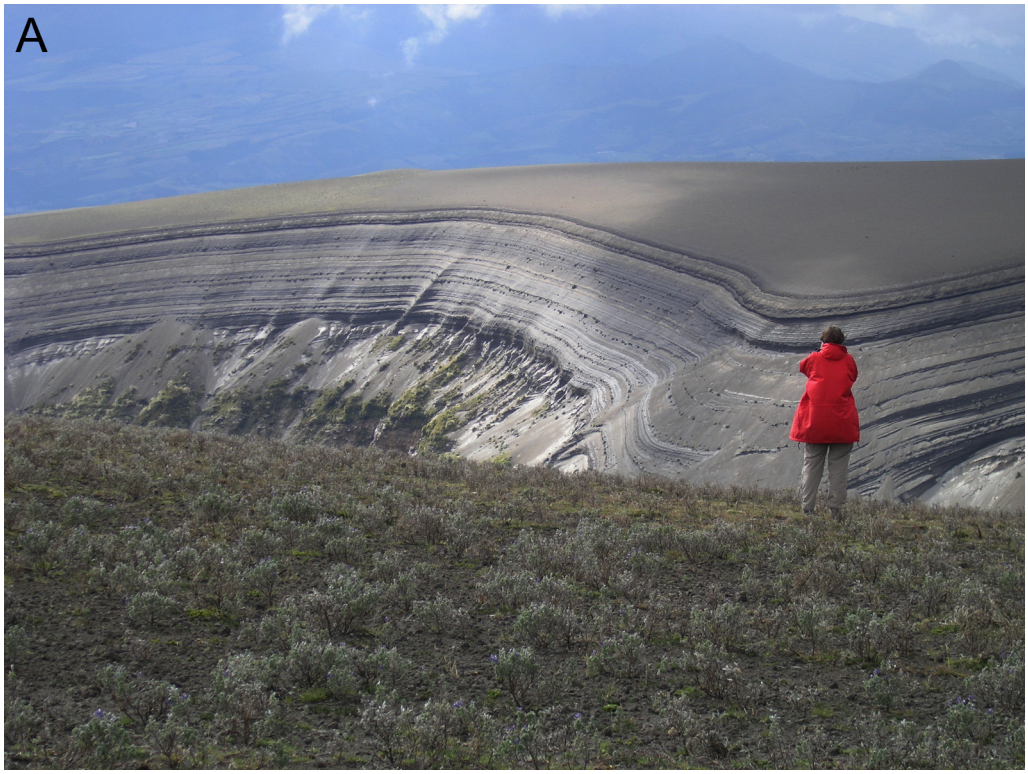
1585

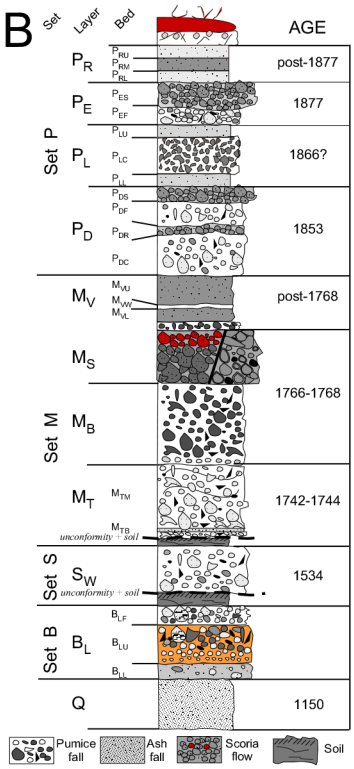
1586 Table 1 The detailed study of the deposits of the different eruptions at a volcano represents
1587 the basis for the reconstruction of the reference eruption scenarios. The table shows the range of
1588 compositional and physical parameters which characterized the explosive activity at Somma-
1589 Vesuvius and that have been used to characterize six different eruptive styles which represent the
1590 reference eruption scenarios for hazard assessment and emergency planning.

1591

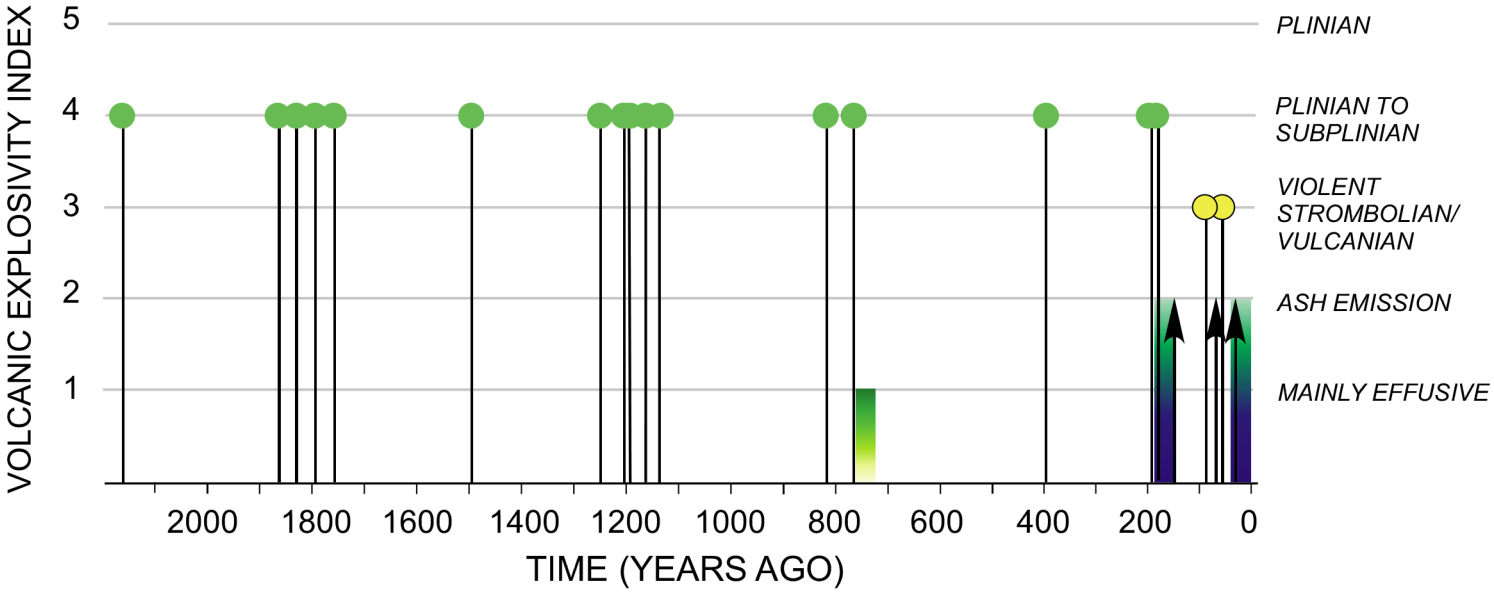
1592


VOLCANIC SYSTEM
PROCESSES
METHODOLOGIES
ERUPTIVE SYSTEM
SHALLOW PLUMBING SYSTEM
INTERMEDIATE STORAGE SYSTEM
DEEP TRANSPORT SYSTEM
MAGMA SOURCE
Eruptive processes
Shallow magma transport, interaction with host-rock
Magma storage, cooling, crystallization and mixing
Deep magma transport, interaction with host-rock
Magma input
Physical volcanology
Geology
Petrology
Experimental petrology & thermodynamic modeling
Crystallization kinetics & numerical modeling

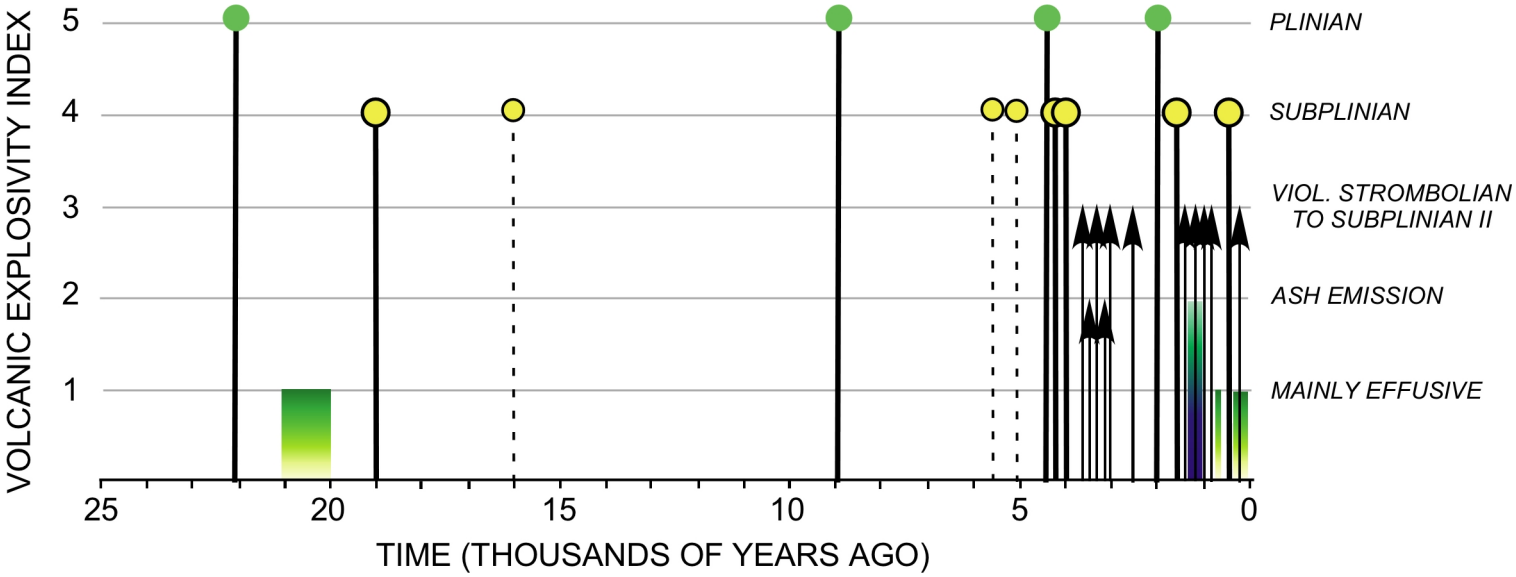

A

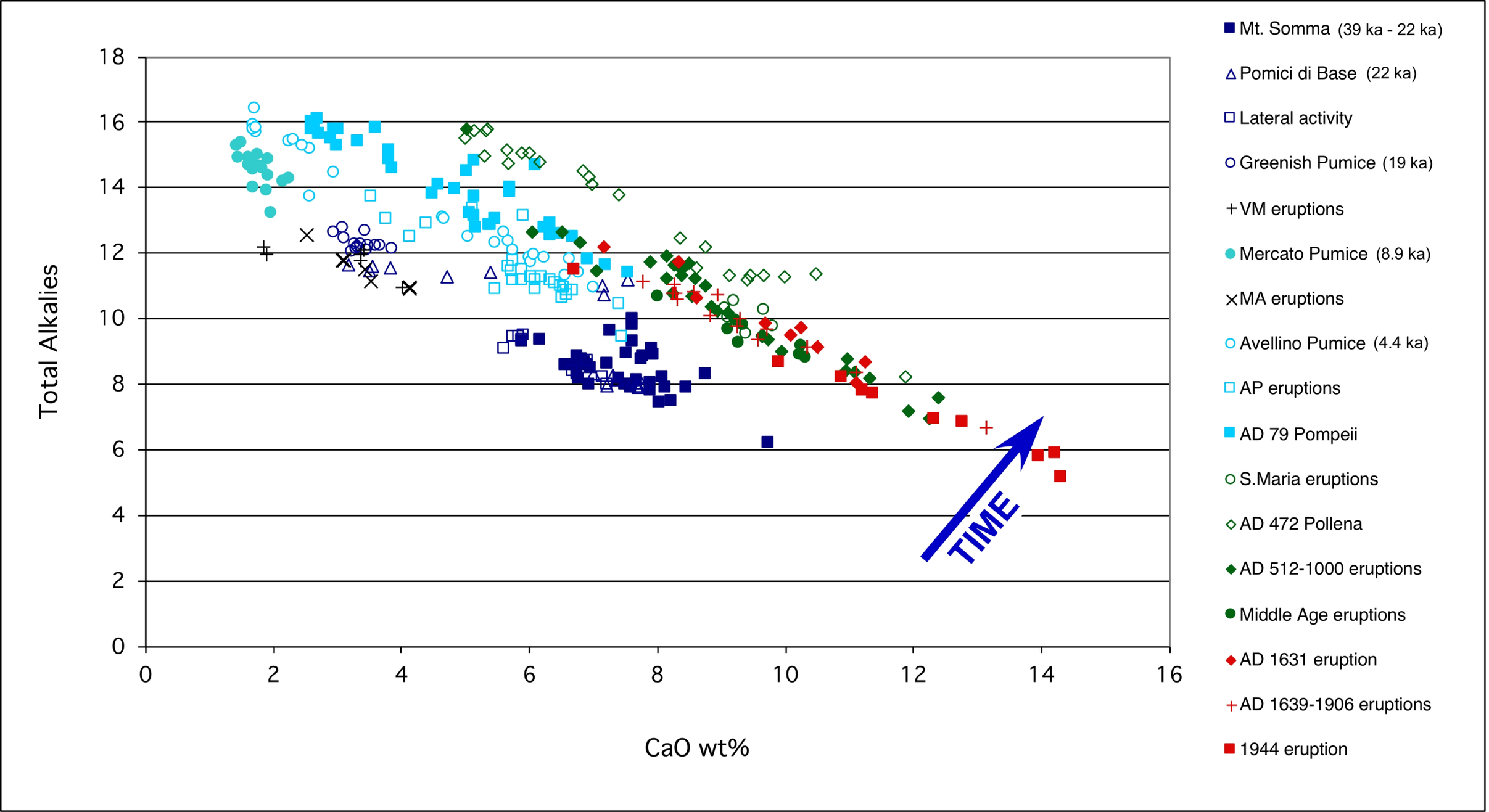

B
Set
Layer
Bed
AGE
Set P
Set M
Set S
Set B
post-1877
1877
1866?
1853
post-1768
1766-1768
1742-1744
1534
1150
unconformity + soil
unconformity + soil
Pumice fall
Ash fall
Scoria flow
Soil

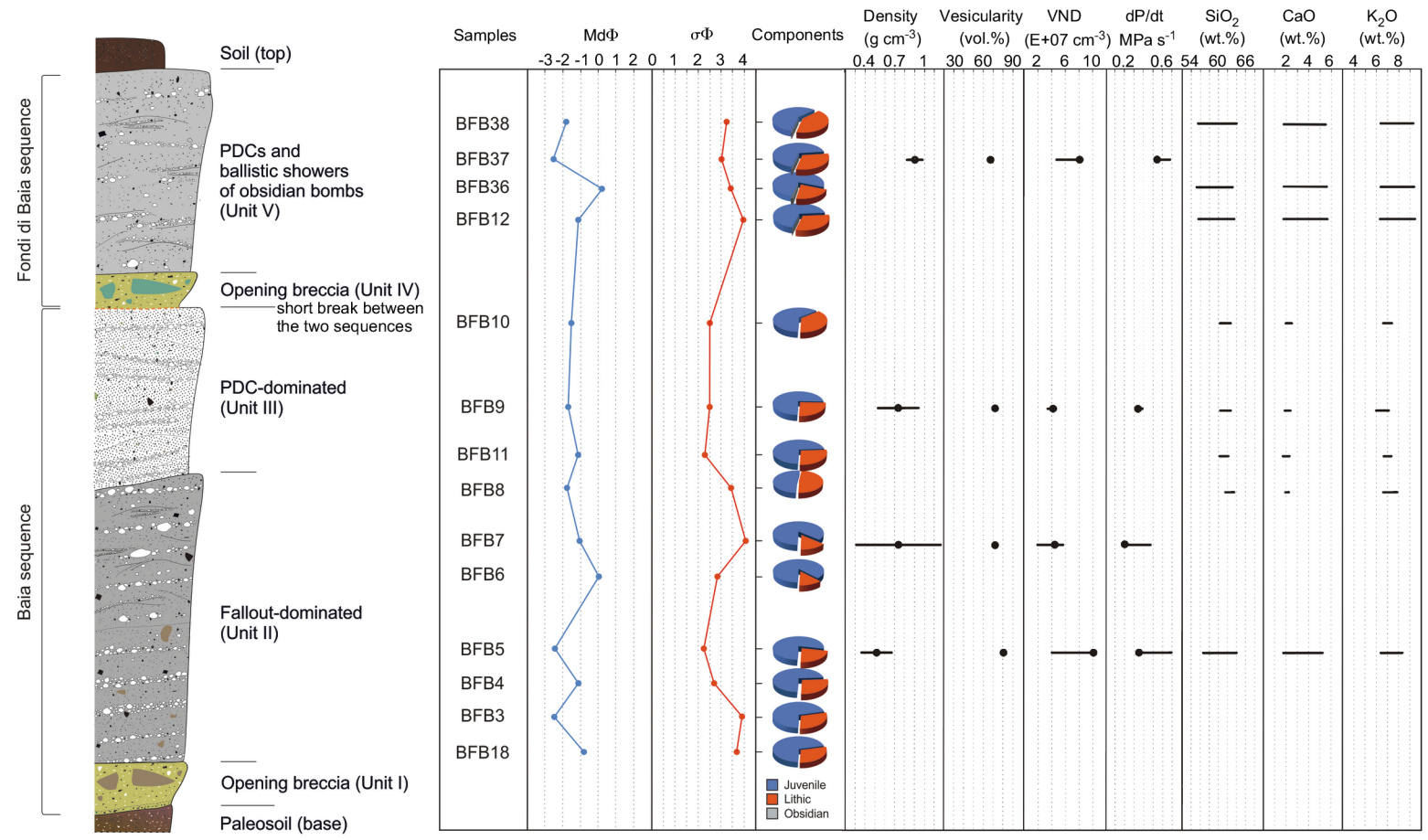
A) ***COTOPAXI***



B) ***SOMMA-VESUVIUS***




Total Alkalies
CaO wt%
0
2
4
6
8
10
12
14
16
18
TIME
Mt. Somma (39 ka - 22 ka)
Pomici di Base (22 ka)
Lateral activity
Greenish Pumice (19 ka)
VM eruptions
Mercato Pumice (8.9 ka)
MA eruptions
Avellino Pumice (4.4 ka)
AP eruptions
AD 79 Pompeii
S.Maria eruptions
AD 472 Pollena
AD 512-1000 eruptions
Middle Age eruptions
AD 1631 eruption
AD 1639-1906 eruptions
1944 eruption


Fondi di Baia sequence
Baia sequence
Soil (top)
PDCs and ballistic showers of obsidian bombs (Unit V)
Opening breccia (Unit IV)
short break between the two sequences
PDC-dominated (Unit III)
Fallout-dominated (Unit II)
Opening breccia (Unit I)
Paleosoil (base)
Samples
MdΦ
-3 -2 -1 0 1 2
σΦ
0 1 2 3 4
Components
Density (g cm-3)
0.4 0.7 1
Vesicularity (vol.%)
30 60 90
VND (E+07 cm-3)
2 6 10
dP/dt MPa s-1
0.2 0.6
SiO2 (wt.%)
54 60 66
CaO (wt.%)
2 4 6
K2O (wt.%)
4 6 8
BFB38
BFB37
BFB36
BFB12
BFB10
BFB9
BFB11
BFB8
BFB7
BFB6
BFB5
BFB4
BFB3
BFB18
Juvenile
Lithic
Obsidian

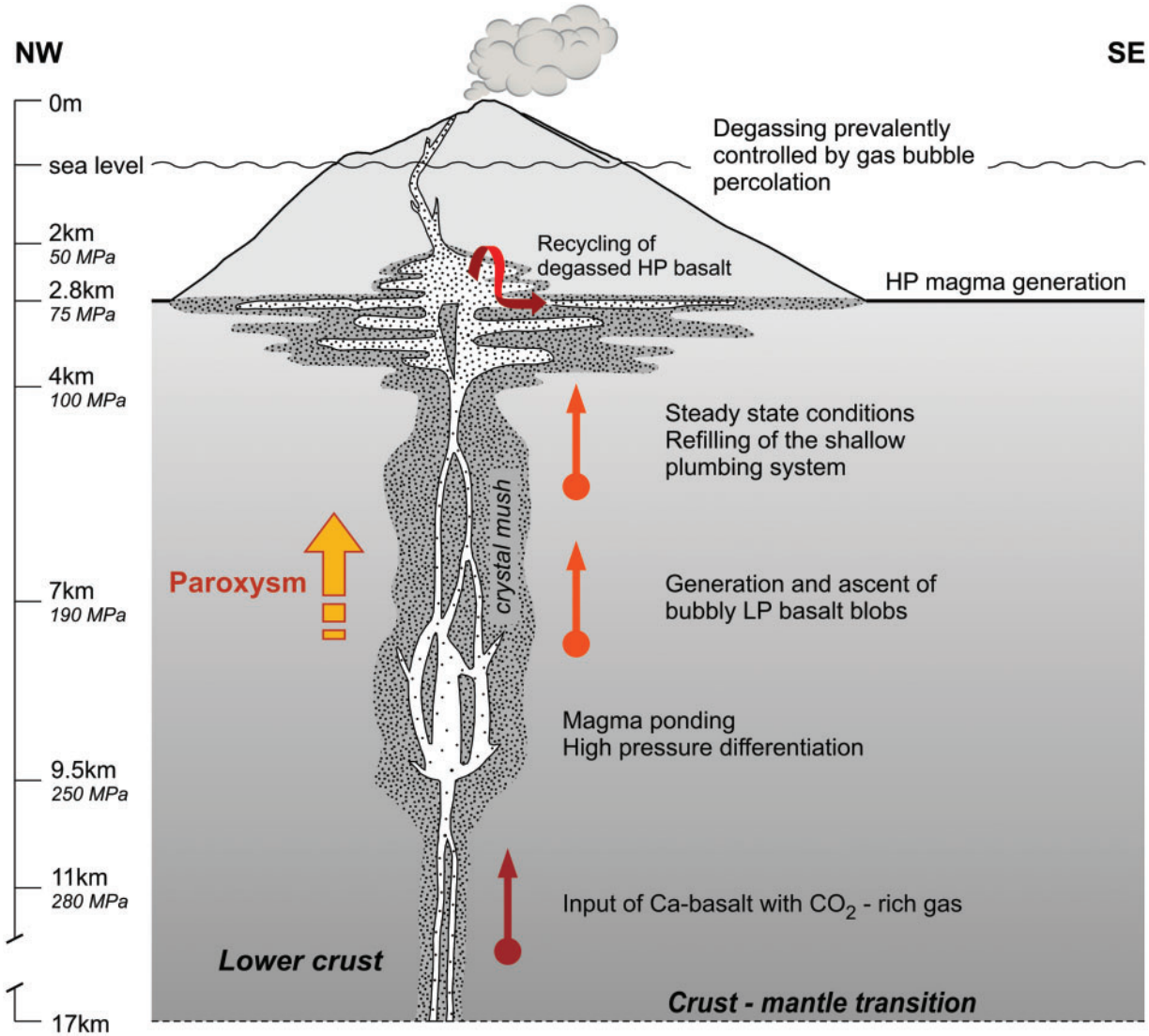


Fig. 10. Interpretative model of the plumbing system of Stromboli based on (1) the melt compositions and melt saturation pressures recorded by sealed melt inclusions and unsealed embayments trapped during olivine crystallization, (2) the crystal textures and (3) the chemistry of Stromboli pumice and scoria samples. The fluid saturation pressures are calculated using Papale *et al.* (2006) and the corresponding lithostatic depth assuming an average density of the surrounding rocks of 2700 kg/m^3. The geometry of the conduits within the uppermost 1 km—imaged as two complex dike systems underlying the summit craters with a sharp change in fracture dip at 80 and 280 m, respectively, below sea level (Chouet *et al.*, 2008)—is oversimplified. LP and HP basalts refer to low- and high-porphyritic magmas, respectively, according to Francalanci *et al.* (2004).

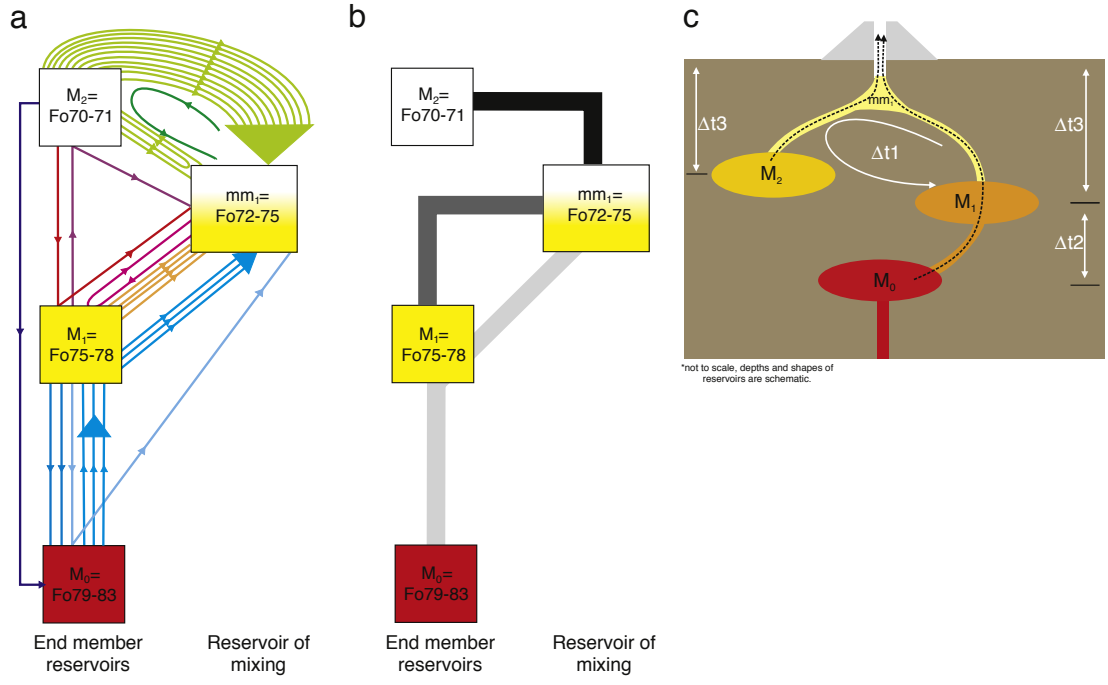


Fig. 4. The plumbing system: (a) Simplified systems analysis of the zoning patterns recorded in olivine crystals erupted between December 1991 and March 1992. Each box represents a magmatic reservoir of different composition identified by the overall core plateau compositions and zoning patterns. M_0, M_1 and M_2 represent end member reservoirs (M_0 = Fo79-83, M_1 = Fo75-78 and M_2 = Fo70-71), whereas mm_1 is a reservoir of mixing. The colored lines represent the zoning patterns recorded in single olivine crystals. The arrows indicate the direction of the zonings from core to rim. All reservoirs are connected with each other. The density of the connection lines can be used to infer the dominant passageways of magma transport. (b) Information distilled from (a) to highlight the three main magma pathways M_0–M_1–mm_1 (light gray bar) M_1–mm_1 (dark gray bar) and M_2–mm_1 (black bar). (c) An example of a physical plumbing system that is consistent with (a) and (b). Other possibilities exist. Locations and connectivity of reservoirs are time integrated, at any given time one or more of these may not have existed. Black dotted lines mark the preferred path followed by many crystals. Various timescales (Δt_1, Δt_2 and Δt_3) that can be extracted from kinetic modeling relate to duration of residence of melts in different segments of the plumbing system, as shown here.

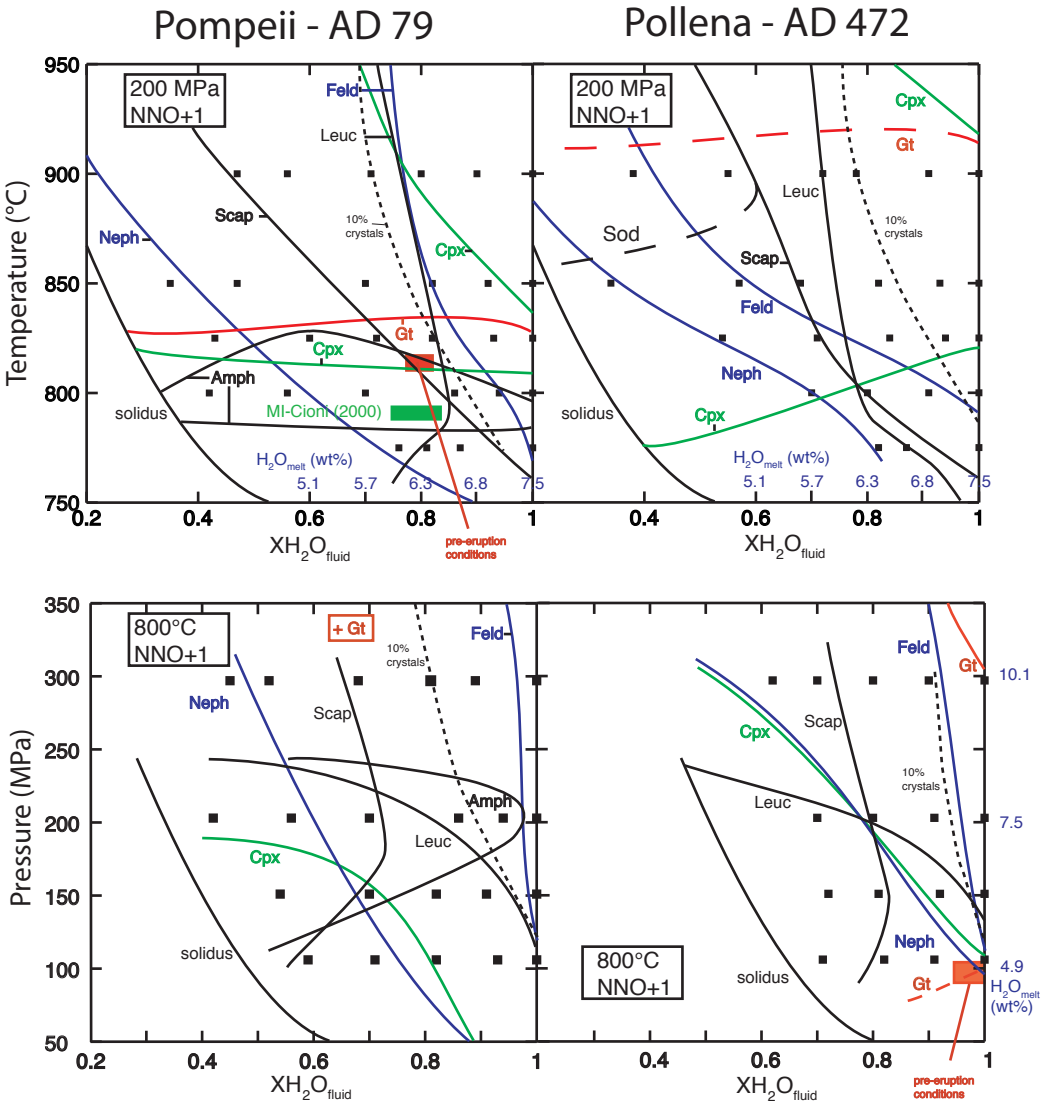
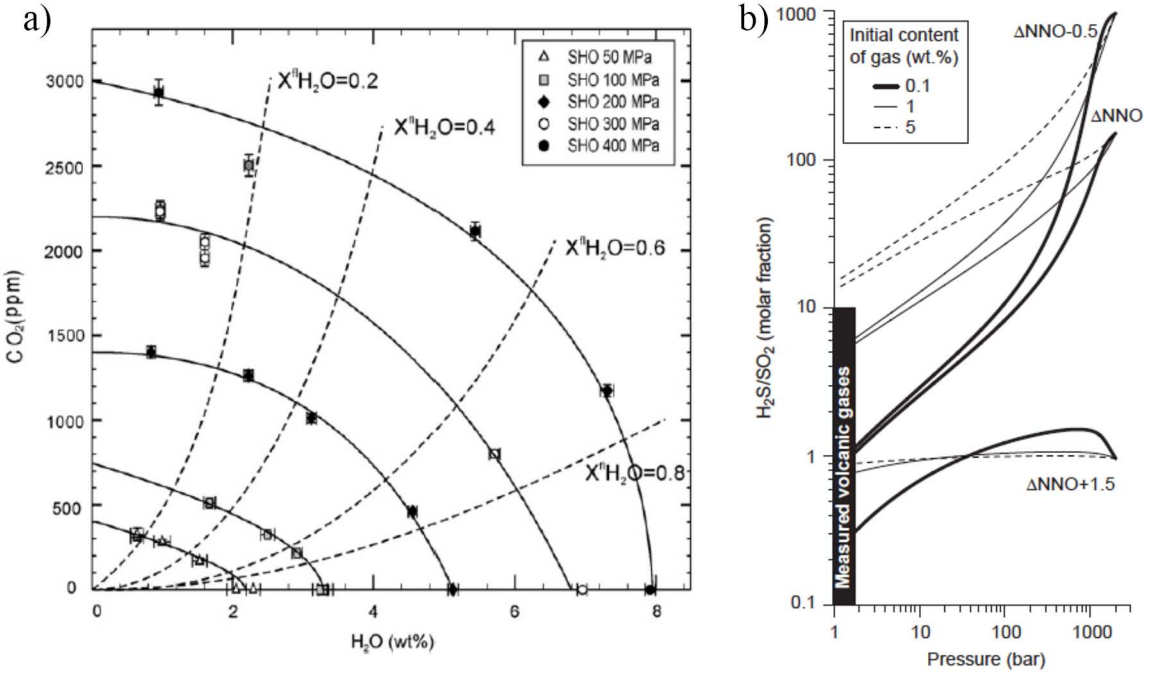
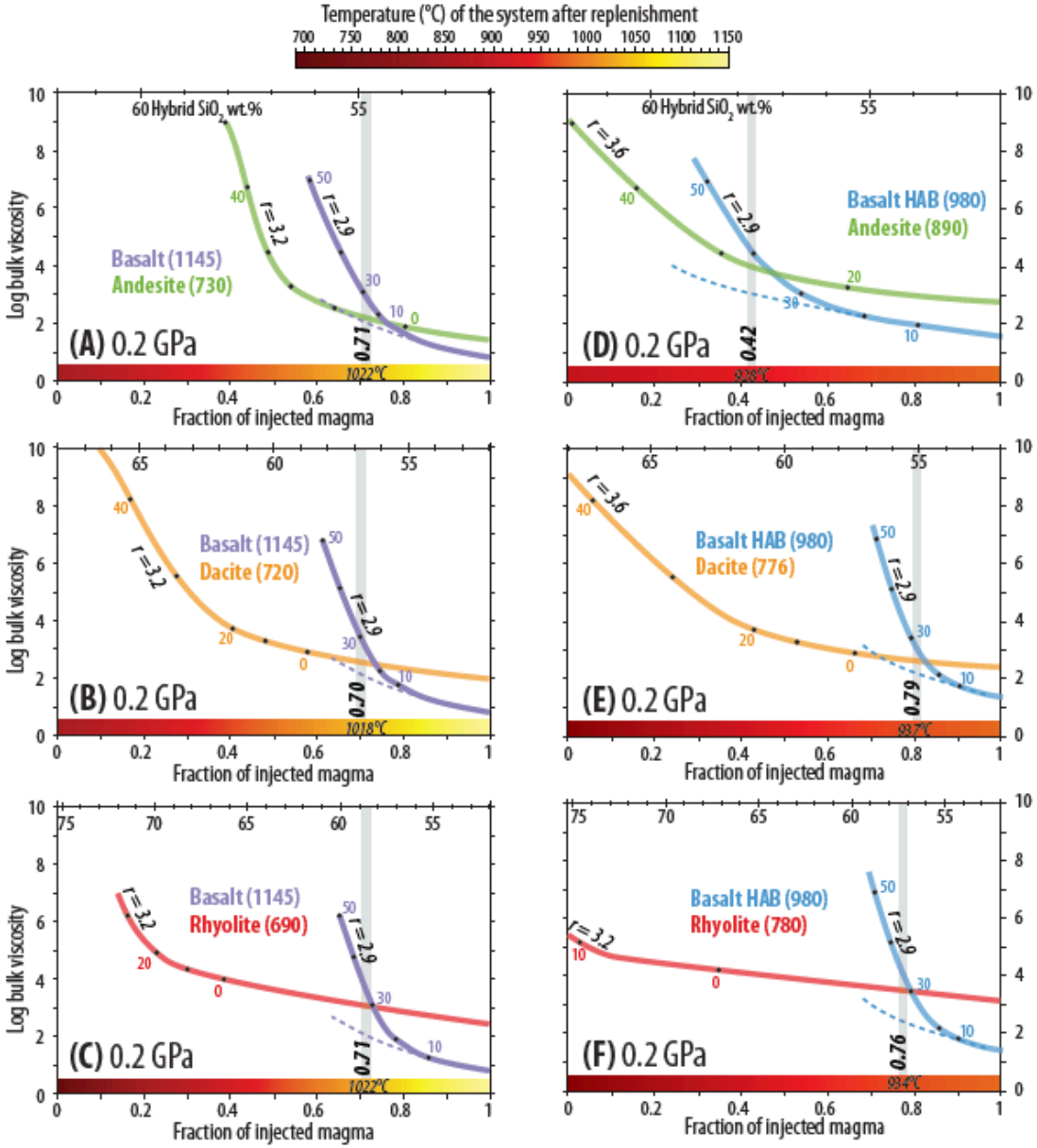
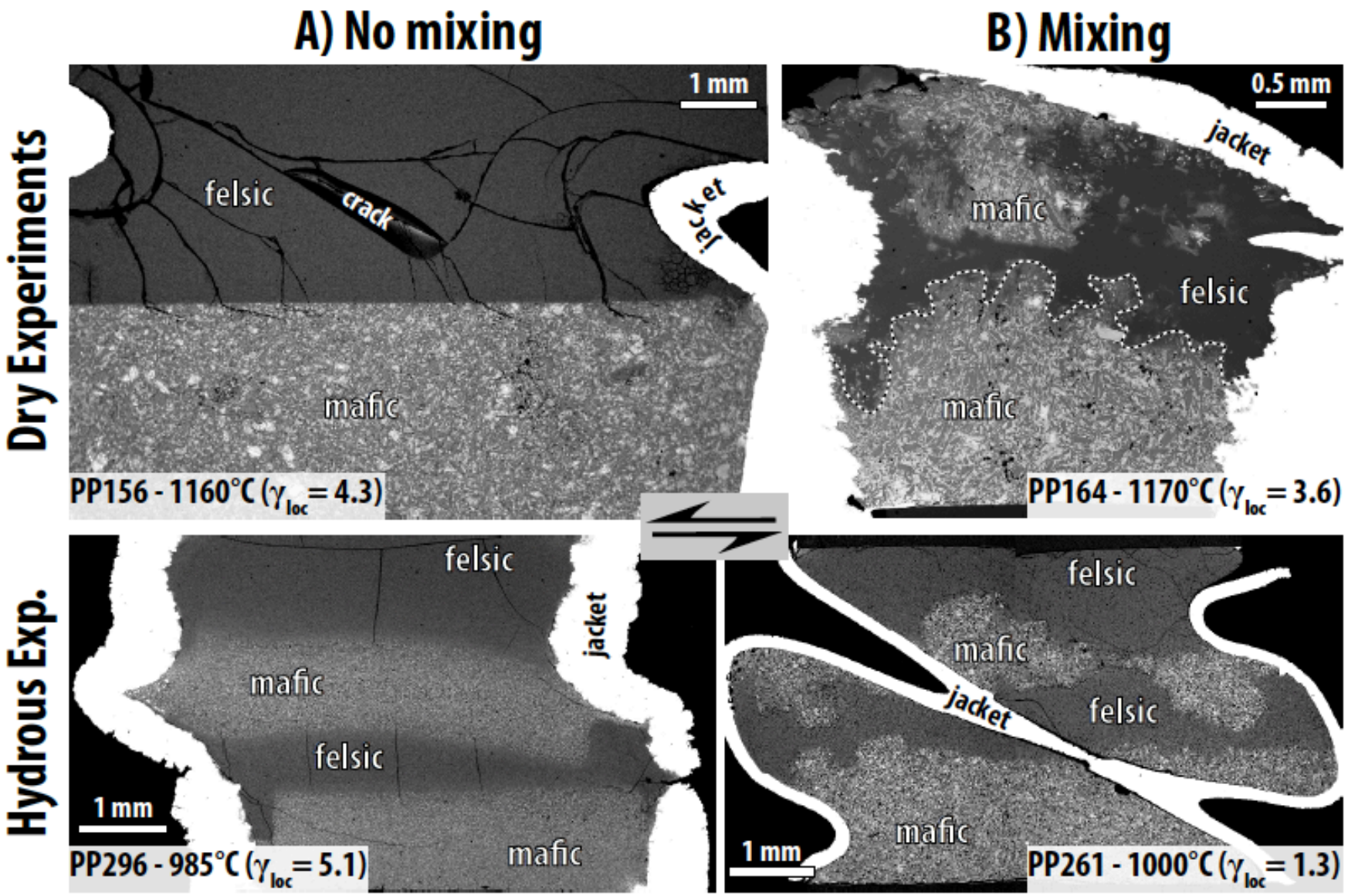
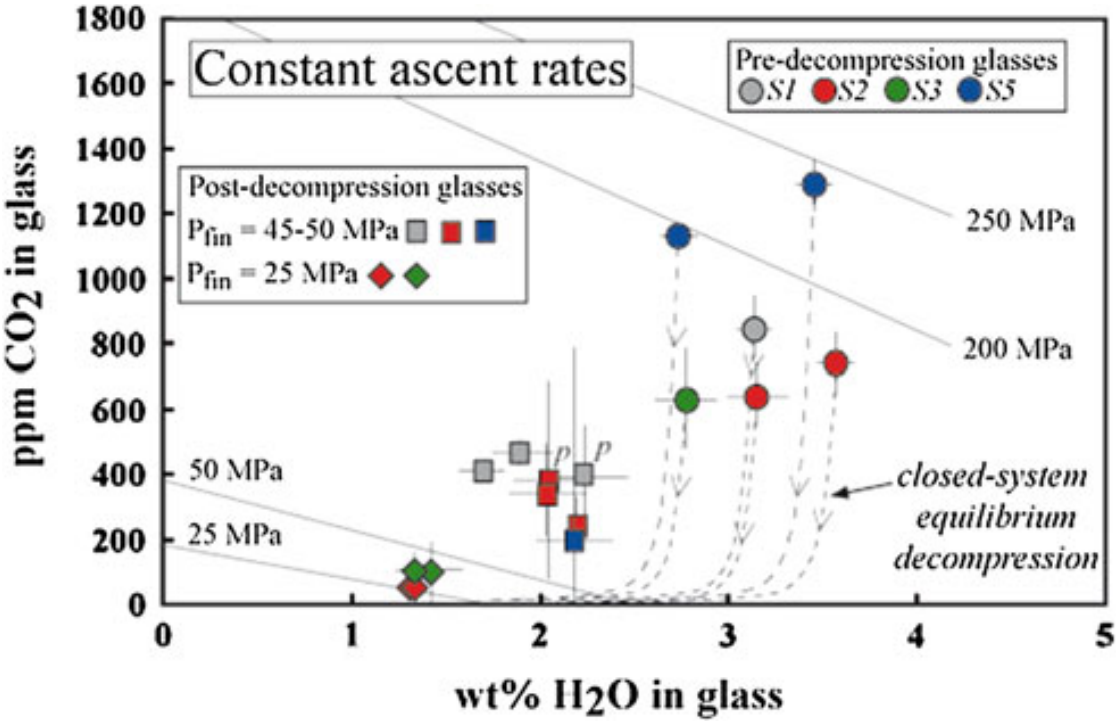

Pompeii - AD 79
Pollena - AD 472
200 MPa
NNO+1
Feld
Leuc
Scap
Neph
10%
crystals
Cpx
Gt
Amph
solidus
MI-Ciom (2000)
H2Omelt (wt%)
5.1
5.7
6.3
6.8
7.5
XH2Ofluid
pre-eruption
conditions
Sod
800°C
NNO+1
+ Gt
10.1
4.9
H2Omelt
(wt%)
Temperature (°C)
Pressure (MPa)

Figure 7.


a)
SHO 50 MPa
SHO 100 MPa
SHO 200 MPa
SHO 300 MPa
SHO 400 MPa
X^fl H2O=0.2
X^fl H2O=0.4
X^fl H2O=0.6
X^fl H2O=0.8
CO2(ppm)
H2O (wt%)
b)
Initial content of gas (wt.%)
0.1
1
5
ΔNNO-0.5
ΔNNO
ΔNNO+1.5
Measured volcanic gases
H2S/SO2 (molar fraction)
Pressure (bar)


Temperature (°C) of the system after replenishment
700 750 800 850 900 950 1000 1050 1100 1150
60 Hybrid SiO2 wt.%
55
Basalt (1145)
Andesite (730)
r = 3.2
r = 2.9
(A) 0.2 GPa
1022°C
0.70
Log bulk viscosity
Fraction of injected magma
60 Hybrid SiO2 wt.%
55
r = 3.6
Basalt HAB (980)
Andesite (890)
r = 2.9
(D) 0.2 GPa
928°C
0.42
Fraction of injected magma
65
60
55
Basalt (1145)
Dacite (720)
r = 3.2
r = 2.9
(B) 0.2 GPa
1018°C
0.70
Log bulk viscosity
Fraction of injected magma
65
60
55
r = 3.6
Basalt HAB (980)
Dacite (776)
r = 2.9
(E) 0.2 GPa
937°C
0.79
Fraction of injected magma
75
70
65
60
55
Basalt (1145)
Rhyolite (690)
r = 3.2
r = 2.9
(C) 0.2 GPa
1022°C
0.70
Log bulk viscosity
Fraction of injected magma
75
70
65
60
55
Basalt HAB (980)
Rhyolite (780)
r = 3.2
r = 2.9
(F) 0.2 GPa
934°C
0.76
Fraction of injected magma


A) No mixing
B) Mixing
Dry Experiments
Hydrous Exp.
1 mm
felsic
crack
jacket
mafic
PP156 - 1160°C (γ_{loc} = 4.3)
0.5 mm
jacket
mafic
felsic
mafic
PP164 - 1170°C (γ_{loc} = 3.6)
felsic
jacket
mafic
felsic
1 mm
mafic
PP296 - 985°C (γ_{loc} = 5.1)
felsic
mafic
jacket
felsic
1 mm
mafic
PP261 - 1000°C (γ_{loc} = 1.3)


Constant ascent rates
Pre-decompression glasses
S1 S2 S3 S5
Post-decompression glasses
Pfin = 45-50 MPa
Pfin = 25 MPa
250 MPa
200 MPa
50 MPa
25 MPa
closed-system
equilibrium
decompression
ppm CO2 in glass
wt% H2O in glass
0
200
400
600
800
1000
1200
1400
1600
1800
0
1
2
3
4
5

Eruption style	*Repose years*	*Volume Km^3*	*Peak MDR $Kg\ s^{-1}$*	*Plume height Km*	*PDC*	*Composition*	*SiO_2 wt%*	*Alkali wt%*	*H2O wt%*	*CO2 ppm*
Plinian ***AD 79, 4400 BP ……***	10^2 - 10^3	10^0 - 10^1	10^7 - 10^8	> 20	Yes	(Trachyte) Phonolite to Teph.-Phonolite	54 – 61 54 – 62	8 – 12.5 11 - 16	5-6 (4400 BP) 6 (AD 79)	0-2000 bdl
Sub-Plinian I **AD 472, 1631 ….**	10^2	10^{-1} - 10^0	10^7	15 - 20	Yes	(Trachyte) Teph.-Phonolite to P-Tephrite	58 - 60 48 - 52	11 – 16 (8 – 12 AD1631)	2.5 (salic) <5 (mafic)	0 – 200 2000
Sub-Plinian II **AP1, AP2, AD 512 …**	10^2	10^{-2} – 10^{-1}	10^6 - 10^7	10 - 15	Minor	Teph- Phonolite to Phon.-Tephrite	48 - 54	8 - 11	No data	No data
Viol. Strombolian **1906, 1944 ….**	10^1 - 10^2	10^{-3} – 10^{-1}	10^5 - 10^6	5 - 10	Minor Avalanching	Tephrite to Phon.- Tephrite	48 - 52	6 - 12	2 - 4	0 - 2000
Ash emission events **AD 79 – 472 period, …**	10^1 - 10^2	Up to 10^{-2} (cumulative)	10^5 (Viol Stromb. Phases) *10^3 (Average)*	< 5	No	Teph-Phonolite to Phon.-Tephrite	49 - 51	9 - 12	1 – 2	0 – 1000
Mild strombolian ***Post 1631 period, …***	*10^0 - 10^1*	*10^{-3}*		No convective plume	No	Tephrite to Phon.- Tephrite	47 – 49	7 - 11	No data	No data